SCHOOL OF POST GRADUATE STUDIES

COLLEGE OF NATURAL AND COMPUTATITONAL SCIENCE

DEPARTMENT OF CHEMISTRY

M.Sc. THESIS

MICROBIAL FUEL CELL WITH GREEN SYNTHESIZED CuO BASED POLYANILINE COMPOSITE AS EFFICIENT BIOANODE MODIFIER CATALYST

BY:

BETELEHEM GUTA

ADVISIOR: Prof. SISAY TADESSE (PhD)

MAY, 2024

HAWASSA, ETHIOPIA

MICROBIAL FUEL CELL WITH GREEN SYNTHESIZED CuO BASED POLYANILINE COMPOSITE AS EFFICIENT BIOANODE MODIFIER CATALYST

BETELEHEM GUTA

A THESIS SUBMITTED TO THE DEPARTMENT OF CHEMISTRY IN PARTIAL FULFILLMENT OF THE REQUIREMENTS FOR THE DEGREE OF MASTER OF SCIENCES IN PHYSICAL CHEMISTRY

HAWASSA UNIVERSITY

HAWASSA ETHIOPIA

MAY, 2024

DECLARATION

I undersigned, declare that this Thesis entitled "**Microbial Fuel Cell with Green Synthesized CuO Based Polyaniline Composites as Efficient bioanode Modifier Catalyst"** is my original work and has not been presented for a degree in any other university, and all sources of material used for this thesis have been properly acknowledged.

Name: BETELEHEM GUTA

Signature: _____

Date: _____

HAWASSA UNIVERSITY

SCHOOL OF GRADUATE STUDIES

ADVISOR APPROVAL SHEET

This is to certify the thesis entitled "**Microbial Fuel Cell with Green Synthesized CuO Based Polyaniline Composite as Efficient Bioanode Modifier Catalyst"** submitted in partial fulfillment of the requirements for the degree of master's science with specialization in physical chemistry, the graduate program of collage of natural and computational science has been carried out by BETELEHEM GUTA under my supervision. Therefore, I recommended that the student has fulfilled the requirements and hence hereby can submit the thesis to the department for defense.

Name of advisor. Prof. SISAY TADESSE (PhD)

Signature _____

Date _____

HAWASSA UNIVERSITY

SCHOOL OF GRADUATE STUDIES

EXAMINER'S APPROVAL SHEET

As member of the Examining Board of the M.Sc. open defense, we officially certify that we have read and evaluated the thesis prepared by BETELEHEM GUTA entitled "**Microbial Fuel Cell with Green Synthesized CuO Based Polyaniline Composite as Efficient Bioanode Modifier Catalyst"** and this is, to certify that the thesis has been accepted in partial fulfillment of the requirements for the degree of Master Science in Physical Chemistry.

Name of Advisor	Signature	Date
Name of Internal Examiner-I	Signature	Date
Name of Internal Examiner-II	Signature	Date
Name of External examiner	Signature	Date
SGS Approval	Signature	Date

Final approval and acceptance of the thesis contingent upon the submission of the final copy of the thesis to the School of Graduate Studies (SGS) through the Department/School Graduate Committee (DGC/SGC) of the candidate's department.

Stamp of SGS Date: _____

ACKNOWLEDGMENTS

Frist of all I would like to thanks Almighty God for his help and protection throughout my life. Next, I would like to express my heartfelt thanks to Professor Sisay Tadesse for his tremendous academic support, valuable suggestions and constructive guidance in writing this thesis with wisdom and patience.

I sincerely express my deepest gratitude to botanist Dr. Firew Kebede for his support to identify *Melia azedarach* plant species and scientific name. And also I would like to extend my deepest gratitude to my associate technical staff Mr. Tilahun Tumiso for providing a pleasant and friendly working environment in the laboratory during experimental work. My sincere gratitude is also expressed to my classmates for their unreserved guidance, encouragement through preparation and organization of my thesis work. I also express my most sincere thanks to my dear friends; Muna Menebere, Remla Sherefa, Tesfahun Eyoel and Biniam Sisay for their always been on my side no matter what and pushing me to go beyond my limits. I obviously cannot nominate everyone, but my gratitude expands to each person who accompanied me in this study, this work is accomplished thanks to you.

Furthermore, I am grateful to express my thanks to Wolaita Sodo University for full sponsorship of my academic education and also Hawassa University Department of Chemistry for accepting me to study my M.Sc. program. Then I would like to thank Adama science and Technology University for their support to characterize my samples. Last but not least, my great and especially thanks to my family for their unwavering moral and financial support.

Table of contents

LIST ACRONYMS

BOD	Biological oxygen demand
CC	Carbon cloth
CCV	Closed circuit voltage
CE	Columbic efficiency
CF	Carbon felt
Cps	Conducting polymer
DMM	Digital multimeter
DCMFC	Double chamber microbial fuel cell
EAM	Electroactive microorganisms
ETR	Electron transfer rate
FT–IR	Fourier transforms infrared
GF	Graphite felt
MECs	Microbial electro genesis
MFC	Microbial fuel cell
NPs	Nanoparticles
OCV	Open circuit voltage
PGEs	Pencil graphite electrodes
PBS	Phosphate buffer solution
PEDOT	Poly (3,4 – ethylenedioxythiophene)
PANI	Polyaniline
PPy	Polypyrrole
PVOH	Polyvinyl alcohol

PD	Power density
PEM	Proton exchange membrane
RVC	Reticulated vitreous carbon
SCMFC	Single chamber microbial fuel cell
SEM	Scanning electron microscopy
TMO	Transition metal oxide
UV- VIS	Ultra violet visible
XRD	X-ray diffraction

LIST OF TABLES

LIST OF FIGURS

ABSTRACT

Microbial fuel cell is a new technology device that converts chemical energy stored in organic waste into electrical energy by using microorganisms as a catalyst with simultaneous waste water treatment. In this study, low-cost phyto-synthesized CuO nanoparticles integrate with conducting polyaniline (PANI) matrix to form CuO/PANI hybrid nanocomposite was synthesized by in situ polymerization methods and PANI was synthesized by oxidative polymerization method. The synthesized sample were characterized through UV-Vis spectroscopy, FTIR, SEM, and XRD, instruments to examine their optical properties, intermolecular bonding and the existence of functional groups, morphology and crystalline structural respectively. Four single chambered microbial fuel cells (MFCs) was constructed with bare pencil graphite anode, pencil graphite anode modified with CuO, PANI, CuO/PANI nanocomposites and PGEs cathode for all four devices. The average crystalline size for CuO NPs, PANI and CuO/PANI NCs was 28.05 nm, 3.2 nm and 20.6 nm respectively. It was found that the maximum open circuit voltage (OCV) obtained by bare PGE, CuO/ PGE,PANI/PGE and CuO/PANI/PGE was 229 ± 11.3 mV, 315 ± 35.3 mV, 485± 15.5 mV, and 630 ± 10.6 mV respectively. The maximum power density and corresponding current density obtained by CuO/PGE, and PANI/PGE have a value 265.75 mWm^{-2} & 2134.34 mA m^{-2} and 387.91 mWm^{-2} & 2418.06 mAm^{-2} respectively. A maximum of 416.01 mWm^{-2}, and 2429.56 mAm^{-2} power density at corresponding current densities was produced by CuO/PANI/PGE respectively. This was 6.3and 4-fold higher in power and current densities than unmodified PGE have values of 65.67 mWm^{-2} and 580.21 mAm^{-2}. From above results modifying anode of MFC with CuO nanoparticles based PANI composite gives a better output as compared with bare PGE in the MFC energy conversion system.

Keywords; Green synthesis, Microbial fuel cell, Anode modification, Electricity generation, Copper oxides nanoparticles, Polyaniline, Nanocomposite.

1. INTRODUCTION

1.1. Background of the study

In recent years, due to the rapid increasing of population numbers consumption of nonrenewable energy sources for vehicle utilization, or other industrial applications leads to the reduction of fossil fuels and its burning produce hazardous pollutants that affect environment and health [1]. Producing alternative energy in the form of bioelectricity and wastewater treatment from organic effluents is the key strategy to minimize energy crises and save the ecosystem [2].To bring off this scientists search for an alternative, attractive, cost effective and ecofriendly technology known as microbial fuel cells (MFCs).

Microbial fuel cell is a device that produces electricity from organic waste matter by using electroactive microorganism (EAM) as a driving force. The concept of MFCs was started throughout the last decade, in 1911, Dr. M. C. Potter -a professor at the University of Durham in the UK- perceived in his series of experiments that the bacteria *E.coli* can generate electricity if put in an organic environment using platinum electrodes. Dr. M. C. Potter could also study about parameters that affect the amount of electricity generated. Those parameters are temperature, concentration, nutrient medium, and so on. The maximum voltage generated was 0.3 to 0.5 volt, and a voltage of this value was never reported in any of the experiments done with microorganism and this makes him the first scientist to exactly prove that bacteria can be result in a current [3]. Microbial fuel cell is designed as double chambers microbial fuel cell (DCMFC) and single chamber microbial fuel cell (SCMFC). The basic components of MFC are anode and cathode electrodes, proton exchange membrane (PEM), substrate and microorganisms. The double chambers MFC contain anode chamber and cathode chamber that separated by proton exchange membrane while in the case of single chamber MFC proton exchange membrane and cathode compartment are not necessary, in this case the anode and cathode electrodes set up in one chamber. In the anode chamber oxidations of organic substance take place under anaerobic condition using bacteria as a catalyst to liberate electrons and proton while aerobic reduction reaction in cathode chamber by exposing it in air and water is formed from combinations of proton, electron and oxygen [4]. MFCs also used in wastewater treatments, since they can convert the organic matter in wastewater into electricity while also removing pollutants. This can increase the ability to maintain in wastewater treatment processes by increasing energy efficiency, reducing additional cost

and emissions of greenhouse gas [4]. The efficiency and economic applicability of generation energy from organic wastes depend on the characteristics and components of the waste materials [5]. Substrate is an important factor in MFCs for any biological process. Acetate and glucose are the most common substrates used as source of carbon for bacterial survive and electron liberated to enhance efficiency and conductivity of the cell. From components of microbial fuel cells, anode electrode plays a vital role on effecincy of the MFCs. The most common anode electrodes used for MFC applications are carbon based materials such as; graphite felt, carbon fiber graphene foil, toray carbon paper, pencil graphite electrodes (PGEs) and so on, due to their cost effectiveness, commercial availability, high thermal stability, ecofriendly, and etc. Apart from those, pencil graphite electrodes (PGEs) is one of the most suitable anode material in MFC due to its biocompatibility, availability, low cost, time saving electrode during surface modifications, electrochemical reactivity, and disposability during its operation [6] [7] [8]. But electrodes from conventional carbon materials are poor in energy conversion and low in wastewater treatment efficiency due to the short-term stability that leads reduction of electron transfer rates between electrodes and bacteria [9].

Electron transfer rate at the biofilm/electrode interface is one of important parameter in evaluating current and power output of MFC's. This can be achieved through selection of specific electrode materials, enrichment with anode-respiring bacteria, or chemical modifications of the electrode surface. This is essential to improve the low electrical conductivity which facilitates the flow of electron and increases speed followed by minimizing bulk electrolyte resistance, low surface area which increases power output, biocompatibility which increase bacterial contact and their respiration process, low stability and durability. The electrode material and morphology should facilitate bacterial attachment and with formation of biofilm. Anode surface chemistry along with the biofilm formation should enhance electron transfer from bacteria to the electrode and play vital role on performance of MFCs [10] [11]. So, modifi cations of anode electrode with low cost, high surface area, highly abundance, and electrokinetic active transition metal oxide (TMO) nanoparticles (NPs) [12] and conducting polymers (CPs). TMO have poor electrical conductivity, poor dispersibility, and low stability in highly protonic media, and also they reduce their long-term electrocatalytic activity in bioenergy production (i.e., reduces the life cycle), bioremediation, and sensing activity [2] [12]. The electrochemical properties of TMO could be improved by incorporating it with conducting polymers. The main advantage of using conduc-

tive polymer in general and PANI especially for anode modifications is to enhance surface area of electrodes for fast electron transfer rate. So, the chemical and mechanical instability in metal oxide is improved by integrating it in PANI to form composites [13]. PANI is a highly conductive polymer and its nanocomposites act as an efficient electrocatalyst to modify anode for performance improvement and wastewater treatment [14]. Many researchers improve anode effecincy by synthesizing metal oxides nanoparticle with conducting polymers as efficient anode modifier catalyst. Dessie *et al.* [13] have synthesized α-MnO_2-based polyaniline binary composite to modify PGEs for high performance microbial fuel cell. Chen *et al.* [15] have prepared MnO_2/polypyrrole Composite to modified anode in marine benthic microbial fuel cells for better electrochemical performance. Nourbakhsh *et al.* [16] have fabricated NiO/ carbon nanotube/polyaniline nanocomposite as bifunctional anode catalyst for high-performance Shewanella-based dual-chamber microbial fuel cell.

Green synthesis method use plant extract or microorganisms (bacteria fungi and algae) as reducing and stabilizing agent in synthesizing of nanoparticle [17]. Copper oxide is a p-type semiconductor with unique properties of good electrical conductivity, large surface area to volume ratio, easily interacts with other particles, good catalytic activity, and less expensive. Copper oxide nanoparticles (CuO NPs) that synthesized by green method is attractive and alternative due to its effective applications in; gas sensor, batteries, catalysis, high temperature super conductors, textile, solar energy conversion tools, and so on [18].

Melia azedarach is medicinal plants that belonging to the Meliaceae family. Phytochemical found in *Melia azedarach* such as:, polyphenols, terpenoids, flavonoids, steroids, acids, saponins, and tannins are used as reducing and capping agent in synthesis of different metal and metal oxides nanoparticles for various applications [19]. In this study CuO NPs is synthesized by using *M. azedarach* leaf extract and composited with polyaniline to modify anode electrodes of MFCs for efficiency improvement.

1.2. Statement of the problem

In recent years the rapid increasing population number leads utilization of fossil fuel as energy source for different purposes. The consumptions of this energy source leads to the reduction of fossil fuel and its burning results emission of carbon dioxide (CO_2) and other hazardous pollutant [1]. The emission of this hazardous pollutant cause global warming that intolerant to ecosystem.

This series problem initiate scientist for searching ecofriendly and cost effective technology known as microbial fuel cell. But the poor efficiency of the device is the main drawbacks for practical applications. In microbial fuel cell the anode electrodes are the major factor that affects efficiency of the device. Material used as electrodes in microbial fuel cell is very expensive and not available easily. Therefore, low cost and easily available carbon conventional material is commonly used in MFC applications. But they are poor in energy conversion and wastewater treatment efficiency due to the short-term stability that cause low electron transfer rates between electrodes and EAM [9]. So, modification of these electrodes with metals/metal oxide nanoparticles like TMO NPs is an alternate technique to increase surface area of electrodes for good electrical conductivity, and also modification with conducting polymers like PANI, PPy is important for better efficiency.

Unlike green synthesis method the other physical and chemical methods has the following disadvantage;- their ease of synthesis was time-consuming and complicated; the use of expensive chemicals with environmentally intolerable solvents that might affect environmental safety, and use of expensive synthesis instruments. A green method is much easier and safer to use, and plant-mediated synthesis of nanoparticles is still a new scheme to be studied [17]. The poor electrical conductivity, poor dispersibility, and low stability in highly protonic media of TMO are reduce their long-term electrocatalytic activity in bioenergy production [2][10] and the conducting polymers swelling and shrinkage behavior in neutral solutions affects the physical strength of the anodes [20]. To address the stated limitations composite of TMO with conducting polymers like PANI as anode modifier catalyst is important for better performance of microbial fuel cell. In recent studies composite of PANI and α-MnO_2 modified PGE gives power density (PD) and current density six and five fold respectively than unmodified PGE [13], Polyaniline-coated molybdenum oxide composite modified carbon cloth (CC) delivered a maximum power density (PD) of 1101 mW/m^2, which was 7.8 times higher than unmodified CC anode [21], Polypyrrole/GO modified graphite felt (GF) anode showed the maximum power density of 1326 $mW\ m^{-2}$ which is 7.9 times higher than unmodified GF anode [22].

Copper oxides (CuO) nanoparticles have gained much attention in electrochemistry especial for anode modification due to its unique properties such as good electrical conductivity, large surface area to volume ratio, ability to promotes electron transfer, easily interact with other particles, good catalytic activity, and low cost [18]. PANI also has a property that makes it preferred

for anode modification such as stability, electrical conductivity, high hydrophilicity, biocompatibility, and etc. In MFC positive charge on PANI and negative charge on bacteria increase the interaction between them and helps to form active biofilm on surface of electrode [21].

To best of my knowledge modification of anode with green synthesized CuO NPs based PANI composite by using *Melia azedarach* leaf extract for MFC performance improvement was not reported so far. In this study *Melia azedarach* leaf extract were used as reducing, and stabilizing agent to synthesize CuO NPs based PANI nanocomposites for modification of low conductivity PGE in single chamber microbial fuel cell to enhance the output of the device or to adders the limitations stated above.

1.3. Objectives

1.3.1. General objective

The main objective of this research work is to study the performance of microbial fuel cell with green synthesized CuO based polyaniline composite as efficient bioanode modifier catalyst by using *Melia azedarach* leaf extract as reducing and stabilizing agent.

1.3.2. Specific objectives

- To synthesize CuO NPs using *Melia azedarach* leaf aqueous extract.
- To synthesize PANI using oxidative polymerization method.
- To synthesize CuO/PANI nanocomposites using in-situ polymerization methods.
- To characterize the synthesized CuO NPs, PANI, and CuO/PANI nanocomposite by using UV-Vis, FT- R, XRD and SEM instruments.
- To construct SCMFC and measure voltage output.
- To evaluate polarization curve and power density curve from synthesized nanomaterials modified anode of SCMFC.
- To compare the power density of SCMFCs with bare PGE and PGE modified by CuO, PANI, and CuO/PANI composites.

1.4. Significance of the Study

This study would describe the advantage of green synthesis of nanomaterials and its modification for anode electrode for performance of MFC through energy production. Also describes the bet-

ter methods to avoid production of unwanted hazardous by product during electricity generation and wastewater treatment through designing attractive, ecofriendly, cost effective MFC. The findings can be used to treat different types of wastewater in different area of the country to lessen environmental pollution and recover energy by utilizing their wastes as a source of energy. Additionally the study would explains the contribution of MFCs to environmental protection since bioenergy is clean energy that is done by breakdown of organic and inorganic wastes and the importance of green synthesis methods of nanoparticles.

2. LITERATURE REVIEW

2.1. Microbial fuel cell

The concept of microbial fuel is begun in 1911 with M. C. Potter, a professor of botany at the University of Durham. In his series of experiments that the bacteria *Saccharomyces* and *Escherichia coli* can produce electricity in an organic environment using platinum electrodes [3]. Microbial fuel cell is a device that converts chemical energy stored in waste materials in to electrical energy by using microorganisms especially bacteria as a catalyst within simultaneous wastewater treatment and nutrient recovery. In waste and wastewater treatment, MFC is effective as it is clean energy, high in performance, and has direct electricity recovery [23]. Microbial fuel cell (MFC) is one of the special fuel cell that is less expensive, ecofriendly, easily designed, and operated at room temperature while other fuel cell is expensive, required complex control system, utilization of complex organic contaminants and produce hazardous pollutants. MFCs are bioelectrochemical systems that can generate electricity via microbial metabolism while removing pollutants such as organic compounds, sulfate, sulfide, nitrate, etc.[24]. Despite having ability to be sustainable technology, there are several challenges in the practicing MFCs for extracting energy from pollutants. The limitations are related with their low power output, slow start-up, and lower efficiencies compared with other technologies [4]. Many process have been passed to improve power generations, those are;- the microbial oxidation of the substrate; electron transfer from the microbe to the anode; electron transfer through the circuit, including the external circuit; proton diffusion from the anode chamber to the cathode chamber; and oxygen supply and reduction at the cathode [25]. Among those processes, the efficiency of electron transfer from the microbe to the anode and oxygen supply and reduction at the cathode have been noted to be the most critical factors that control the power density and waste treatment efficiency of MFCs. Electricity generation from MFC can stimulate the microbial oxidation of the pollutants. Therefore, improving the power density is one of the greatest challenges for the practical applications of MFCs [24].

2.2. Working principle of microbial fuel cell

Microbial fuel cell is a device that produces electricity by using electrons derived from biochemical reactions catalyzed by bacteria. The device contains anode chamber, cathode chamber, elec-

trodes, proton exchange membrane and an external circuit for completed circuit. In the anode compartment, microbes are degrading organic wastes under anaerobic conditions, which oxidize substrates and produce electrons, protons, and other metabolites. The electrons released by the microbes are collected by the anode and passes through an external circuit to the cathode which uses oxygen as electron acceptor. The reduction of oxygen to water is achieved by the transfer of electrons and protons at the cathode chamber [26]. For each electron passed, one proton is carried through the membrane to reach the cathode [27]. Figure 1 depicts operating principles of microbial fuel cell.

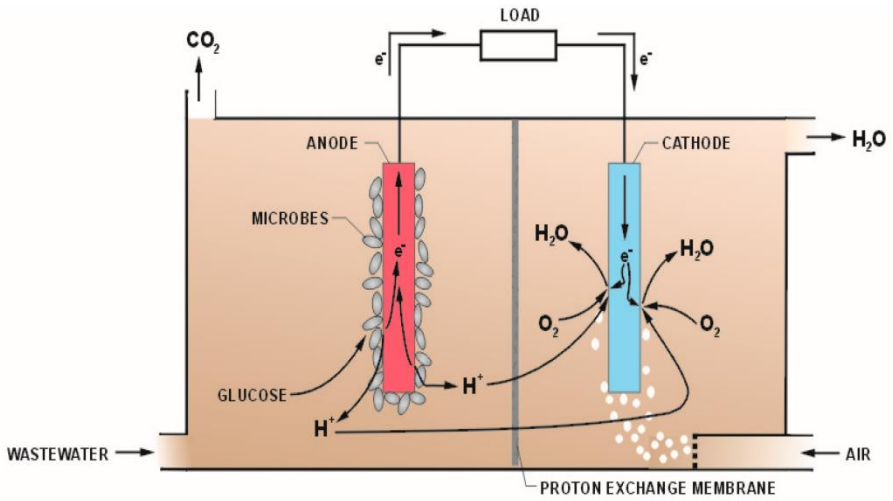

Figure: **1** Operating principle of microbial fuel cell [28].

Anodic reaction

$$C_6H_{12}O_6 + 6H_2O \rightarrow 6CO_2 + 24H^+ + 24e^- \quad (a)$$

Cathodic reaction

$$6O_2 + 24H^+ + 24e^- \rightarrow 12H_2O \quad (b)$$

Overall reaction

$$C_6H_{12}O_6 + 6O_2 \rightarrow 6CO_2 + 6H_2O + \text{Electricity} \quad (c)$$

2.3. Types of microbial fuel cell

Microbial fuel cell is classified in to two depending on the mechanism of microorganisms can transport electron to anode; mediator and mediatorless [26].

2.3.1. Mediator microbial fuel cell

In mediator type of MFCs, microorganisms are not responsible for transporting electrons to the anodic surface because they do not synthesis a protein with active sites to help them do that. Instead, they use chemical mediators or agents that are also called “electroactive metabolites” to transfer electrons between the microorganisms and the electrode at relatively higher concentrations [23]. Mediators play an important role in electron transport for those microbes that are unable to transfer the electrons to the anode. During the process of electron transfer, the mediators inter the cell and accept the electrons before liberating them and donating them to the anode as the final electron acceptor. At this point, the mediator is oxidized back to its initial state after depositing its electrons [23]. In contrast to endogenous mediators, synthetic exogenous mediators are toxic to microorganisms and expensive. The toxicity and instability of synthetic exogenous mediators (dyes and metal organics) limit their applications in MFCs [29]. Therefore, the application of MFCs with endogenous mediators produced by microorganisms such as sulfide, iron, pyocyanin, etc., is advantageous in wastewater treatment and power generation [30]. Mediators are usually methylene blue, neutral red, thionine, methyl viologen and humic acid [31].

2.3.2. Mediatorless microbial fuel cell

Mediatorless microbial fuel cells use electrochemically active bacteria instead of mediator to transfer electrons to the electrode (electrons are carried directly from the bacterial respiratory enzyme to the electrode). Among the electrochemically active bacteria are, *Shewanella putrefaciens, Escherichia coli, Aeromonas hydrophila*, and others are common in mediatorless MFC. Mediatorless MFC are a more recent area of research due to the factors that affect optimum efficiency, such as the strain of bacteria used in the system, type of ion-exchange membrane, and system conditions (temperature, pH, etc.) are particularly well understood. Mediatorless microbial fuel cells can, besides running on wastewater, also generate energy directly from certain plants [32]. This configuration is known as a plant microbial fuel cell. Common plants include reed sweet grass, cord grass, rice, tomatoes, lupines and algae [32]. In the plant-MFC, plants and bacteria were produce electricity by converting solar energy into green electricity. The great concept of plant MFC is that plants produce rhizodeposits, mostly in the form of carbohydrates, and the bacteria convert these rhizodeposits into electrical energy via the fuel cell [33].

2.4. Design of microbial fuel cell

There are two configurations of microbial fuel cell. Those are single chamber microbial fuel cell (SCMFC) and double chambers microbial fuel cell (DCMFC). The designs of the device have a great factor on working efficiency of it. Both design of microbial fuel cell contain anode and cathode electrodes made from different material with membrane or being membraneless for proton transfer.

2.4.1. Single chamber microbial fuel cell (SCMFC)

Single chamber microbial fuel cell as the name indicates it is one compartment MFC in which anode and cathode electrodes are in one chamber by eliminating proton exchange membrane and cathodic chambers. One compartment MFCs offer easy scalability, simpler designs and cost savings [34]. The cathode is directly in contact with air and no membrane or separator required in a single-chamber MFC while the waste substance used as separator. They are quite simple to scale up than the double chambered fuel cells and thus have found extensive utilization and research interests lately. Nevertheless, the absence of a membrane in a single-chamber MFC have several limitations: the additional substrate consumption for oxidation process since the produced electrons might be consumed by oxygen that limit electron amount to generate electric current, and the electrolyte might be mixed, this reduce the efficiency of the device [35]. Figure 2 below illustrate schematic diagram of single chamber microbial fuel cell.

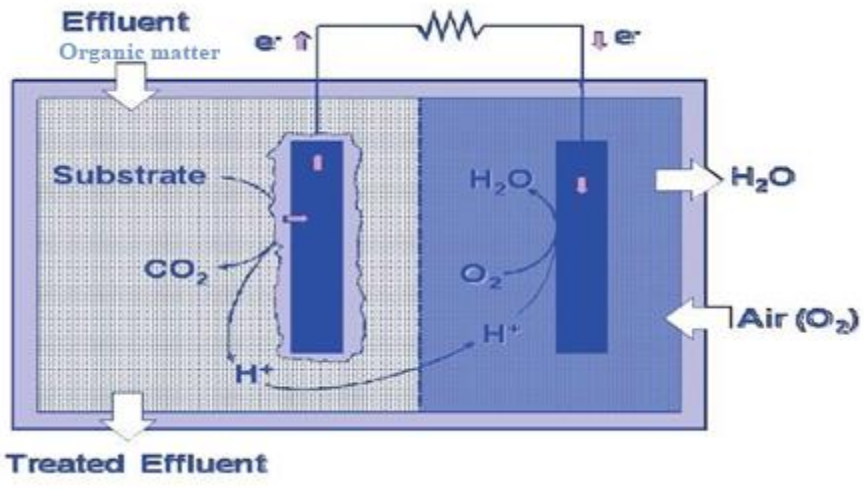

Figure **2** Schematic diagram of single chamber microbial fuel cell [36]

2.4.2. Double chambers microbial fuel cell (DCMFC)

This MFC configuration is the most widely used and consisting of anodic chamber, and cathodic chamber separated by the proton exchange membrane which mainly functions as medium for transfer of proton to complete redox reactions. The anode chamber is kept oxygen free for anaerobic breakdown process to occur, which is usually purged with nitrogen. The electrodes in both chambers can connect to external wires and the wire in to digital multimeter for voltage measurements. It can be a suitable designed to scale up for treatment of large volume wastewater and other waste contain carbon. The most used MFC in basic experiments is the one with two chambers, resembling a galvanic cell. Although the H-type or dual-chambered microbial fuel cells is the most common in laboratory use, but it is the most challenging to scale up due to the impractical configuration, and expensive materials [34]. Double-chamber MFCs have the ability to generate a high voltage output and power density as compared to single chamber microbial fuel cell [35]. Figure 3 below shows schematic diagram of double chamber microbial fuel cell.

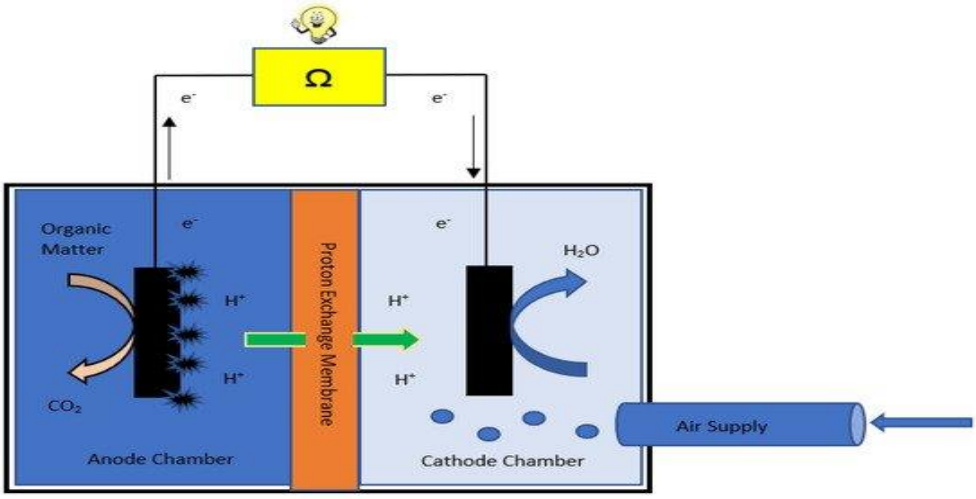

Figure **3** Schematic diagram of double chamber microbial fuel cell [37].

2.5. Basic component of microbial fuel cell

The basic components of microbial fuel cell are:

- Anode chamber and cathode chamber contain anode and cathode electrodes respectively
- Proton exchange membrane
- Substrate
- Microorganisms

Table 1 Basic components of microbial fuel cell [34]

Component	Materials	Remarks
Anodes	Graphite, graphite felt, carbon paper, carbon-cloth, Pt, Pt black, reticulated vitreous carbon(RVC)	Necessary
Cathodes	Graphite, graphite felt, carbon paper, carbon-cloth, Pt, Pt black, reticulated vitreous carbon(RVC)	Necessary
Anodic chambers	Glass,polycarbonate,Plexi glass	Necessary
Cathodic chambers	Glass,polycarbonate,Plexi glass	Optional
Proton exchange membrane (PEM)	Nafion, Ulterx, polyethylene. Poly(styrene-codivinyl ben-zene):, salt bridge,porcelain septum or solely electroltye	Necessary
Electrode catalyst	Pt, Pt black, MnO_2, Fe^{3+}, pol-yaniline, electron mediator immobilized on anode	Optional

2.5.1. Electrodes

Anode and cathode electrodes are the main parts of MFCs. They play a vital role on efficiency of MFC especially anode. The usage and applicability of anode and/or cathode electrode materials leads to selective priority for MFCs. The electrode materials are mainly carbon-based (e.g., graphite rod or plate, carbon cloth, carbon paper, carbon felt), and metal-based (e.g., stainless steel copper mesh, and platinum) materials. For use in MFCs, they should be biocompatible, conductive, porous, easily made at low cost, recyclable, scalable, possess high specific surface area, corrosion resistance, high mechanical strength, and suitable for bacterial growth [38]. In

microbial fuel cell low cost electrode materials are alternate for practical applications than highly efficient electrode materials (i.e. platinum) due its high rice disadvantages [39].

2.5.2. Proton exchange membrane

The performance of MFC depends on the microbial activity in the anodic chamber and the efficient migrations of the protons into the cathodic chamber. In this manner, the membrane acts as a boundary between the anaerobic anode chamber and aerobic cathode to prevent undesired mixing of species between chambers [37]. The membranes are run in batches and can be used for producing higher power output and can be utilized to give power in much inaccessible conditions. The membrane should also facilitate transportation of only H^+ ion from anode to cathode and switch the passage of negatively charged particles and O_2 from cathodic to the anodic chamber [37]. The most important proton exchange membrane that alternate for MFCs is the Nafion ionomer due to its high proton conductivity. But its high price limit it for practical experment, instead low cost proton exchange membrane used for MFCs technology.

2.5.3. Substrates

Substrates are nutrient sources of electrons, and microorganism's to generate electricity and conduct their metabolic respiratory activity. The most important substrates used for microbial fuel application are acetate and glucose. The efficiency of the cell also depends on the type of the substrate used; mainly its voltage, power densities, and Columbic Efficiency (CE). Usually, for experimental purposes, organic substrate can be alternate to evaluate the efficiency of organic matter in MFCs [5].

- **Acetate** is ion found in acetic acid. This compound is a source of carbon and it can prompt electroactive microbes. The compound also applicable in the modified versions of microbial fuel cell like Microbial electrogenesis cells (MECs) at room temperature [5].
- **Glucose** Adding glucose to wastewater sludge enhances the conductivity property of the cell. But, when compare with acetate it yields low regardless to columbic efficiency. In a double chamber MFC, the energy columbic efficiency was 42% for acetate and 3% for Glucose which is due to fermentation that glucose is subject to in the presence of various microorganisms and this cause a loss of electron [5].

2.5.4. Microorganisms

Microorganisms are living things that used as a biocatalyst in microbial fuel cell for degradations of organic matter. MFC converts chemical energy in a bio-convertible waste matter, directly into electricity by using bacteria as driving force. The bacteria can be switch from electron acceptor such as oxygen or nitrate to achieve the desired electricity. This type of bacteria is called Exo-electrogens, "exo-"for exocellular and "electrogens" related to the ability to directly transfer electrons to a chemical or material that cannot accept electron [40]. Exoelectrogenic bacteria are fit with MFCs function due to their activity and ability to transport electrons outside of the cell and can be found in a number of places. According to *Du et al,* they are found in soil, marine sediment, waste substance, fresh water sediment and activated sludge [34]. There are two types of microorganisms (gram-positive and gram-negative) that used in MFC. Gram-positive micro-organisms in MFC are Clostridium butyricum, Saccharomyces sp., and others, Gram-negative microorganisms used in MFC are Bacillus violaceus, Escherichia coli, Pseudomonas fluorescens, Proteus vulgaris, Pseudomonas methanica, Desulfuromonas acetoxidans, Geobacter sulfurreducens, Methylovorus dichloromethanicum, Methylovorus mays, Shewanella putrefaciens, and etc. [41]. The most important electrochemically active microorganisms used in MFC are, *Shewanella putrefaciens* [42], *Escherichia coli* [43], and *Geobacter sulfurreducens* [29].

2.6. Application of microbial fuel cell

MFCs are responsible for various applications such as electricity generation, wastewater treatment, biosensor, hydrogen production and etc.

2.6.1. Electricity generation

Electricity generation is the primary application of microbial fuel cell technology. MFCs are capable of converting the chemical energy stored in the waste matter in to electrical energy with the aid of micro-organisms [40]. The microorganisms play an essential role in the oxidation reactions occurring at the anodic chamber that responsible for organic matter decomposition and releasing electrons and protons. The anodic chamber contains a substrate (synthetic or a real wastewater) and a single or a mixed culture of microorganisms. The protons are released to the anolyte and pass through proton exchange membrane by diffusion while the electrons are collected by the anode electrode and pass through external wire to produce electric current [44]. The

current and power density produced from microbial fuel cell is increased by modification of electrodes since modifications minimize the internal resistance and start-up time of the system. Electrodes are modified with metal catalyst/nanoparticles/chemicals, conductive polymer, and nanocomposite to increase the outputs. The cathode is also modified to alternate the expensive platinum catalyst with a cheaper one having the same properties [45]. MFCs with MoO_2/PANI/CC anode delivered a maximum power density (PD) of 1101 mW/m^2, which was 7.8 times higher than unmodified CC anode electrode [21], PPy/MnO_2 modified CC anode delivers a power density of 2139.7 ± 17.5 mW m^{-2} which is 3.58 folds higher than that with bare CC anode [46], PPy/GO modified GF anode showed the maximum power density of 1326 mW m^{-2} which was significantly larger than that associated with the unmodified GF anode (166 mW m^{-2}) [22].

2.6.2. Wastewater treatment

Wastewater treatment is also potential application of microbial fuel cell. MFCs can be used to treat wastewater simultaneously as it can convert the organic matter in wastewater into electricity while also removing pollutants. When organic waste is decomposed by microorganism there is a breaking down of pollutants and generating of electrons that flow through an electrical circuit to the cathode compartment with simultaneous generation of clean water as a byproduct, which can be reused or released back into the environment. MFCs provide a more energy-efficient alternative to traditional wastewater treatment plants, as they meet the energy needs of wastewater treatment plant by generating electricity from the organic matter in wastewater [4]. Wastewater treatment systems have different series processes with specific functions which contribute to cleaning the waste as it passes through different stages. The primary stages include aerobic biological processes which use both oxygen and food in order survives bacteria. The biodegradable soluble organic contaminants are consumed by bacteria and wastewater treatment can be successfully [47].

2.6.3. Hydrogen production

Instead of electricity hydrogen is produce when MFCs device can be modified. Under normal operating of MFC, the protons released during anodic oxidation reaction pass through membrane to the cathode and from water by combine with oxygen in cathodic chamber. The production of hydrogen from protons and electrons released from metabolism of microbes in an MFC is thermodynamically impossible [40]. But applying additional potential might be overcome this unfa-

vorable reaction. In biohydrogen production the cathodic reaction must be anaerobic which reduce the efficiency of the MFC. Hence, the device is modified to develop Microbial electrolysis cells (MECs) which combine electrochemistry with bacterial metabolism. The reaction mechanism is similar to that of MFCs; bacteria decompose organic waste into CO_2, electron and proton. The released electron pass through electric circuit from anode and proton pass through membrane are combining at the cathode to form the desired hydrogen by applying external potential [48].

2.6.4. Biosensor

Microbial fuel cell is used as a biosensor for the detection of organic matter and toxic pollutants in the wastewaters during electricity generation. In biosensor the energy of organic matter is converted to signals by aid of transducers. The transducers are not required in MFC since the device itself acts as transducer, utilizing bacteria to generate signals in the anode and the material of electrodes is used as transducers [45]. MFCs based biosensor have various applications, including monitoring microbial activity, testing biological oxygen demand (BOD), detection of toxicants, detection of microbial biofilms that cause biocorrosion and some other unusual application [49]. MFC-based biosensors the detection of toxicity applicable in turn-off or inhibition mode which means the presence of toxic substance minimize the electrical signals generated by system. The metabolic activity of the exoelectrogens is decrease because of the toxin concentration added to the anolyte and this affect the power output of the system. The toxicity of substance after detection is calculated by comparing the toxin concentration and electric signal output with simultaneous measurement of current change (I) and amplitude of output signal or inhibition ratio (IR). In MFC biosensors the bioanodes are expect to affect the sensitivity of toxic agent, but modification of both anode and cathode electrodes are for minimizing the response time and amplifying the capacity of detection. For example , optimizations of potential at anode by using potentiostat can be used to maintain the sensitivity of the MFC biosensor and the cathode working also affect the amplitude and the output signal precision [45].

2.7. Electrode materials

Electrode materials that can serve as both anode and cathode in MFC devices should be meet the following criteria; good electrical conductive, inexpensive for practical application, high porosi-

ty, non-corrosive, suitable for bacterial growth. The various suitable electrode materials are metal-based (e.g platinum, copper) due to high conductivity and superior mechanical properties and carbon- based (pencil graphite electrode, carbon cloth, carbon felt and etc.) due their excellent microbial adhesion, light weight, high porosity, high specific surface area, good chemical, mechanical and thermal stability, tunable electronic properties, and low cost. Since metal based electrode materials are expensive and not commercial available carbon based are the common one [50]. However electrodes from conventional carbon materials are poor in energy conversion and low in wastewater treatment efficiency due to the short-term stability results for sluggish electron transfer rates between electrodes and bacteria, modification with most conductive and high-quality materials such as metal oxides NPs, conducting polymer and nanocomposites is required [9].

2.7.1. Pencil graphite electrode

Pencil graphite leads used as working electrodes are currently known as pencil graphite electrode (PGE) used as electrode components in microbial fuel cell. Due to its low cost, easy to use, eco-friendly, more convenient and there is no time-consuming electrode surface cleaning step, and good sensitivity viewed it as selective electrode materials in microbial fuel cell technology. To improve its electrochemical activity and sensitivity modifying it with transitional metal oxides, conducting polymer or composite of the two is very beneficial [7].

2.8. Anode electrode role in MFC performance

Anode in MFC is a place where waste materials degradable anaerobically by action of microbes especially bacteria to produce electricity and plays a vital role on performance of MFC. Conventional carbons, metal/metal oxides, and conducting polymers are the most common electrode materials to build anode in MFC operation [13]. The carbon derivatives are most often used as anode electrode due to its excellent electrons transfer kinetics, cost effectiveness, good biocompatibility, and reasonable chemical activity, mechanical and thermal stability. Poor performance of anode electrode in MFC is still a major drawback for its practical applications. Successful anode electrode modification is expected to enhance the MFC electricity generation efficiency. Conventional carbon (stainless steel, graphite electrode, carbon cloth), conducting polymers, and metal oxides, have been employed as anode electrode modifiers with different degree of success [51].

2.9. Transition metal oxide catalyst in MFC performance

Transition metal oxides are used for modification of poor conductivity and low electrocatalytic electrodes in microbial fuel cell. Its excellent structural dynamicity, environmental friendship during synthesis and nontoxicity properties makes TMOs is unique and selective for electrode modification. Among transition metals the oxides of (Mn, Co, Fe, Cu, Ni and etc.) mainly responsible for modification purpose. In particular, transition metal oxides due to having unpaired d-orbital electrons on their structure enabling their electrochemical catalysis activity in MFC [21]. But there are some limitations related to TMOs, in protonic media such as its low stability, poor dispersibility, and electrical conductivity. So, they required further modification with other novel and active nanomaterials like conducting polymers [20].

2.9.1. Copper oxide (CuO) nanoparticles

The unique and phenomenal properties that can be exhibit by metal/metal oxides nanoparticles make them a subject of great interest. The metal oxides nanoparticles are widely selective for different application since; they exhibit properties like good electrical conductivity, large surface area, chemically reactive, and small size. Copper oxide (CuO) are considered as an alternate to various categories of metals oxides due to its cost-effectiveness, economically attractive and promising, nontoxicity and easy preparation [52]. It is the simplest copper compounds with low band gap in range of 1.9 - 2.1 eV and exhibits useful physical and chemical properties, such as high temperature superconductivity, electron correlation effects, stability, easily react with polarized liquid and polymers, and etc [53]. Copper oxide nanoparticles (CuO NPs) is the p-type semiconductor appear as a brownish-black powder, have low band gap, attractive, and interesting material [54]. Copper oxide nanoparticles (CuO NPs) synthesized by different methods with extremely high surface areas and unusual crystal morphologies have attracted huge attention due to their applications as water purifiers, in gas sensor, batteries, catalysis, magnetic storage media, solar energy conversion tools, and so on [18]. Different parts of herb extracts have been used for the preparation of copper oxide nanoparticles for various applications, namely, CuO NPs synthesized from *Cassia fistula* and *Melia azedarach* leaf extracts for eradication of multidrug resistant Klebsiella pneumonia and Helicobacter pylori biofilms [55], CuO NPs synthesized from *Mint leaves* and *orange peels* extracts for lead, nickel, and cadmium removal from contaminated water [56], CuO NPs synthesized from *Parthenium hysterophorus* leafs extract for degradation of ri-

fampicin antibiotic [57], CuO NPs synthesized from *Banana Peel* Extract for photocatalytic degradation of Congo red (CR) dye [18], and so on. The Figure 4 below depicts formation of CuO NPs by using plant extract.

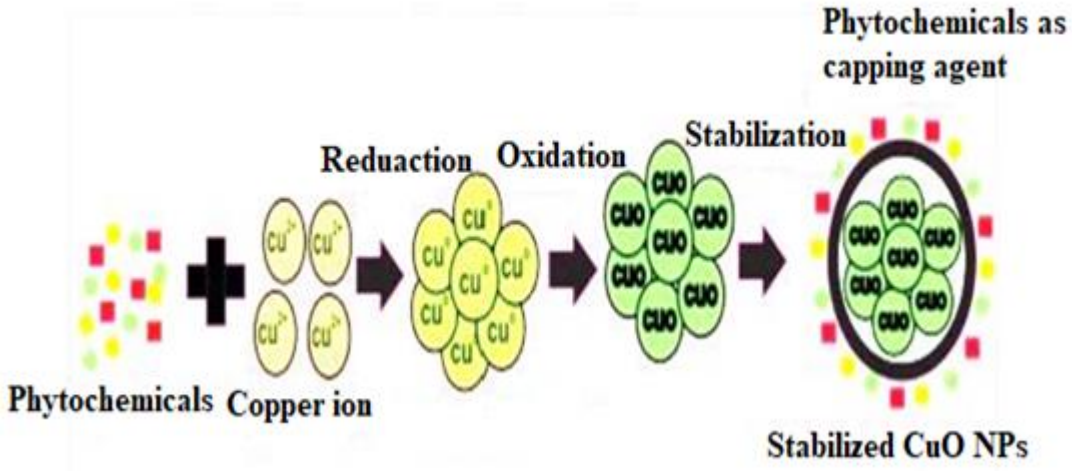

Figure: **4** Mechanism for formation of copper oxide nanoparticles [58].

2.10. Conducting polymers role in MFC performance

The variety of conducting polymers (polyaniline (PANI), polypyrrole (PPy), poly (3, 4 - ethylenedioxythiophene) (PEDOT), polystyrene and etc.) are used for anode electrode modification in MFC. The conjugated double bonds along the backbone of the polymer allow the movement of electron along polymer chain and it is a key property that made the polymer a good electric conductor [59]. Conducting polymers are good materials that have high conductivity, have catalytic behavior, good electrochemical activity, and easily synthesized process make them highly coating materials in MFC manufacturing [14]. CPs commonly used for charging a storage battery, semi-conducting applications and various applications of conducting polymers especially to modify the required electrode in MFC performances can be increased by doping with other functional materials like metal/ metal oxides to form polymer composites since its different properties, like thermal stability, mechanical properties, conductivity, and corrosion protection properties can be improved by doping [60].

2.10.1. Polyaniline (PANI)

Polyaniline (PANI) is an interesting and attractive polymer in electrochemical due to its good electronic conduction, low cost, simple synthesis process, excellent chemical and environmental stability [61]. It is a good electrical conductor when used as electrode by coating on low conductor electrode materials. The positive charge on PANI backbone, interact with negatively charged of EAM outer cell membrane to form a conductive biofilm on electrode surface. This is due to strong adhesion of more EAM coliforms on polymer coated bare electrode materials [62]. In addition to provide a protective function for bacteria the conductive polyaniline also used as catalyst in electrochemical cell in order to improve of the device. But its poor electrical conductivity, poor dispersibility, and low stability in highly protonic media, the swelling and shrinkage behavior limits its practical applications. To overcome this problem doping it with metal oxides or deposit on electrode materials to increase the number of catalytic active sites is recommended [61].

2.11. Copper oxide based polyaniline (CuO/ PANI) nanocomposite

Composite material is combination of two or more than two of chemically distinguish materials with clear separating interface and shows properties that achieved by all components [63]. Nanocomposites are kind of composites in which at least one of the components shows dimensions in the nanometer range (1-100 nm) [64] These nanomaterials are suitable alternatives to solve limitations of micro composites. The inorganic composite at nanoscale have high surface to volume ratio and have significant value in modifying the electrical, optical, and dielectric properties of polymer. In synthesized polymer/inorganic nanomaterial the formed nanocomposite have a synergetic properties between polymer and inorganic material [65]. This nanocomposite if formed when metal and metal oxide particles have been incorporated into the conductive polymer [63]. The PANI-CuO nanocomposites exhibit hybrid properties that reflected from both PANI and CuO such as good electrical conductivity, thermal stability, large surface area, and so on [63]. The PANI-CuO nanocomposites has various application in different application area; from those few of them are; PANI-CuO nanocomposite find application in microwave frequencies as absorbing and shielding materials [66], PANI-CuO nanocomposite used as Anticorrosive with tunable electrical properties for broadband electromagnetic interference shielding [67], PANI-CuO nanocomposite used as antifungal agents against *Aspergillus parasiticus* [68] . In this work green

synthesized PANI-CuO nanocomposite was coated on pencil graphite electrode to improve power output of microbial fuel cell.

2.12. Copper oxides and its composite in microbial fuel cell

Copper oxides nanoparticles and it composites have a vital potential in improving the efficiency of microbial fuel cell due to their unique properties such as good electrical conductivity, large surface area, stability and durability. Copper oxides and it composite facilitate the transfer of electrons to improve the power output and enhance the oxygen reduction reaction (ORR) to achieve higher current densities and better overall performance. Previous several studies have investigated the role of copper oxides and it's composite in MFCs by modifying low cost electrodes materials. For example copper oxides nanoparticles coated on carbon nanofibers anode for better performance in a microbial fuel cell [69], Nano copper oxide-modified carbon cloth as cathode for microbial fuel cell [70], Graphite cathode modified with CuO/ ZnO for efficiency improvement of MFCs [71], Mixed transition metal oxides of nickel and copper (Ni and Cu), supported on a graphene (NiO–CuO/G) electrocatalyst, were synthesized and tested as a cost effective cathode for ORR in MFCs [72], Activated graphite/CuO composite were prepared as cathode in algae assisted microbial fuel cell [73] and etc.

2.13. Green synthesis of nanoparticles

Basically, nanoparticles are synthesized by two ways , known as the 'top-down' approach (lithography, mechanical, thermal ablation, chemical etching and etc.) and 'bottom-up' approach (electrospinning, sol-gel, hydrothermal, green approach and so on). In the top-down approach, nanoparticles are synthesized by size reduction of bulk material into fine particles where as in bottom-up approach the atoms, molecules and are joined to form nanoparticles [74]. From bottom-up approaches green synthesis method is a one that uses plant extract or microorganisms (bacteria fungi and algae) as reducing, capping and stabilizing agent in synthesizing of nanoparticles. Due to its easy handling, easy accessibility and synthesis, cheapness, compatibility with the biomedical applications, non- toxicity byproducts, save time, ecofriendly to produce nanoparticles at large scale compare to bacteria and/or fungi mediated synthesis plant extract was more selective than other green methods [17].

2.14. Plant extract role for metal oxides nano particles synthesis

By using green synthesis method plants; leafs, roots, seed, bark, flowers, fruits and etc. are used as reducing and stabilizing agent to synthesis nanoparticles of metal/metal oxides from their precursor. Plants extract has ability to reduce and stabilize metal oxides nanoparticles in single-step synthesis using phytochemicals present in it. Phytochemicals present in different part of plant extracts that used as reducing and stabilizing agents are alkaloids, sugars, flavonoids, saponins, steroids, terpenoids, tannins and so on [74]. These phytochemicals is used to reduce metal ion and minimize the agglomeration of NPs as it is used as capping agent [75]. For example Flavonoids contain various functional groups, which have a great ability to reduce metal ions. During tautomeric transformations the enol in flavonoids is converted in to keto-from in order to release the reactive hydrogen atom. The reduction of metal ions into metal nanoparticles is realize the process, and also the other biomolecules found in plant extracts that are responsible the formation of metal/metal oxides nanoparticles is sugars source such as glucose and fructose [17]. Figure 5 shows the general steps for obtaining phytochemicals from plants.

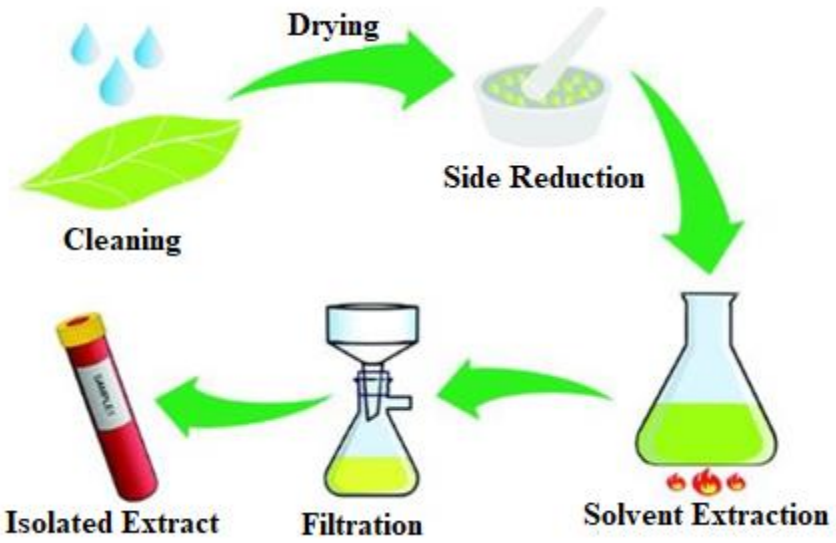

Figure: **5** Schematic diagram shows general steps for obtaining phytochemicals from plants [76].

2.14.1. *Melia azedarach* Plants

Melia azedarach also known as chinaberry Indian is a deciduous tree species belonging to the Meliaceae family [19]. It is common trees in Southeast Asia, Northern Australia, many African and Arab countries. *Melia azedarach* plants are fast-growing and high-quality trees that contrib-

uted in plant pesticide. From its species the mahogany one is responsible in manufacturing agricultural implements, furniture, and plywood. *Melia azedarach* is also greatly applicable in health care and pharmaceutical industries, since it is used as analgesic, anticancer, antiviral, and antimalarial [77]. The tree also used to absorb harmful and toxic gas in urban green area [78]. Different parts (fruits, seeds, leaves, bark, roots, and stems) of the plant can be used as medicine for treatment of leprosy, scrofula, nau-sea, vomiting, dermatoses, expel worms, and skin disease [79]. The leaves and fruits are responsible as anthelmintic and antifeedant towards insects [80][19]. Extracts from the leaves, fruits, and seeds of *Melia azedarach* have been found in medicinal and pesticide properties against various pathogens and pests, respectively [81][82]. The phytochemical found in different parts of *Melia azedarach* pant *are* polyphenols, terpenoids, flavonoids, steroids, acids, anthraquinone, alkaloids, saponins, and tannins [83][84]. Leaves of this plant are bipinnate (twice compound that has a central stem with small leaves ordered on either side of it) and rich with biomolecules that required for nanoparticles synthesis [19]. Aqueous extracts of *Melia azedarach* are used as reducing and stabilizing agent in synthesis of different metal and metal oxides nanoparticles for various applications [19]. From those some of them are; ZnO NPs were synthesized by using leave extract of *Melia azedarach* for microbiological applications [85], Ag NPs were synthesized by using leave extract of *Melia azedarach* for enhancement of antidiabetic, wound healing, and antioxidant Activities [86], MgO NPs were synthesized by using *Melia azedarach* seed extract for Larvicidal and antioxidant activities [19]. Figure 6 shows *Melia azedarach* plant trees.

Figure: **6** *Melia azedarach* plant trees [83].

3. MATERIALS AND METHODS

3.1. Chemicals and Reagents

The fresh and healthy *Melia azedarach* leaves and wastewater sludge was collected from Hawassa University main campus Hawassa, Ethiopia. Copper sulphate pentahydrate ($CuSO_4.5H_2O$) purity ≥ 99%, Sigma-Aldrich], aniline (($C_6H_5NH_2$) 99.5% Merck), ammonium per sulphate (APS; ($(NH_4)_2S_2O_8$) 98%, Sigma-Aldrich), ethanol (C_2H_5OH) 98%, Merck), hydrochloric acid ((HCl) 37%, Merck) chemicals was used as a received. All the necessary chemicals, and substrate used for MFC test was analytical grade and used as a received. The required solutions for this study were prepared from distilled water.

3.2. Instruments and Apparatus

Electric grinder was used for making powder. Electronic balance (Sartorius AG. Germany) was used for weighing gram of precursor salt, plant leave and nanomaterials powder. Oven (INSIF, India, Ho 13301) and muffle furnace (INSIF, India, Ho) was used for drying and calcinating purpose respectively. Digital Multimeter (DMM, Model: mY- 63) was used for measuring voltage output of MFC. Decade resistance box, Beaker, copper wire, pH meter, measuring cylinder, HB pencil graphite(Camlin, China) , Whatmann filter paper (No.1, India), magnetic stirrer, hot plate, test tube, round-bottom flask, Refrigerator (SM-480, Germany), was used for multipurpose.
UV-Vis Diffuse reflectance spectroscopy (JASCO V-670 UV –Vis), X-ray diffractometer (XRD-7000, Shimadzu Corporation, Japan model), Scanning electron microscopy (SEM) (JEOL - JSM-IT300L), and Fourier transforms infrared (FT-IR) spectra Perkin Elmer FT-IR BX spectrophotometer was used to observe absorption spectra and maximum wavelength, crystal phase information, surface morphology, and intermolecular bonding vibration and stretching motion of synthesized CuO NPs, PANI and CuO/PANI nanocomposites respectively.

3.3. Materials synthesis

3.3.1. Preparation of *Melia azedarach* leaf extract

Melia azedarach leaf extract was prepared according to literature obtained from literature [87], with little modification. The collected *Melia azedarach* leaves were washed with tap water and then again with distilled water to remove dusts and unwanted particles. Then the leaves were dried at room temperature for 5 days. The dried leaves were grinded by using electric grinder to

obtain fine powder. After that 20 g of *Melia azedarach* leaves powder was weighed and taken in to round-bottom flask. Then 200 mL of distilled water was added and heated for 1/2 hr at 80 ^{o}C with stirring using magnetic stirrer. Then the solutions was allowed to cool for 1 hr and filtered two times by using filter paper (No.1, India) to obtain *Melia azedarach* leaf extract. Finally, it was stored in refrigerator at 4 ^{o}C for further use. Figure 7 below shows flow chart for preparation of *M. azedarach* leaf extract.

Figure: **7** Flow chart for preparation of *M. azedarach* leaf extract.

3.3.2. Synthesis of CuO NPs by using *Melia azedarach* leaf Extract

CuO NPs was synthesized according to literature [88] with little modification. Briefly, 25g of copper sulphate pentahydrate ($CuSO_4.5H_2O$) was weighed and dissolved in 1000 mL of distilled. Then 20 mL of aqueous leaf extract was vigorously mixed with 80 mL of copper salt solutions and heated for 4 hr at 80 ^{o}C with addition of NaOH to adjust pH on magnetic stirrer hotplate until a black colour paste was obtained, and cooled it at room temperature. Finally, the paste-like product was scratched and calcined in a muffle furnace at 400 ^{o}C for 2 hr, yielding black-colored powder. The biosynthesis of pure CuO NPs can be explained through equations (d-g), which represent the probable mechanism involved in the process;

Cu^{2+} + Plant extract → [$Cu^{2+/}$Plant extract] (Initiation) (d)

[$Cu^{2+/}$plant extract] → [Cu/Biomolecules] (Reduction) (e)

[Cu/Biomolecules] → (NaOH)/Stir→ [CuO/Biomolecules] (Oxidation (f)

[CuO-Biomolecules] → stir/(at 80 ^{o}C)→ CuO NPs (stabilization) (g)

Figure 8 depicts flow chart for green synthesis of CuO Nanoparticles by using *Melia azedarach* leaf extract.

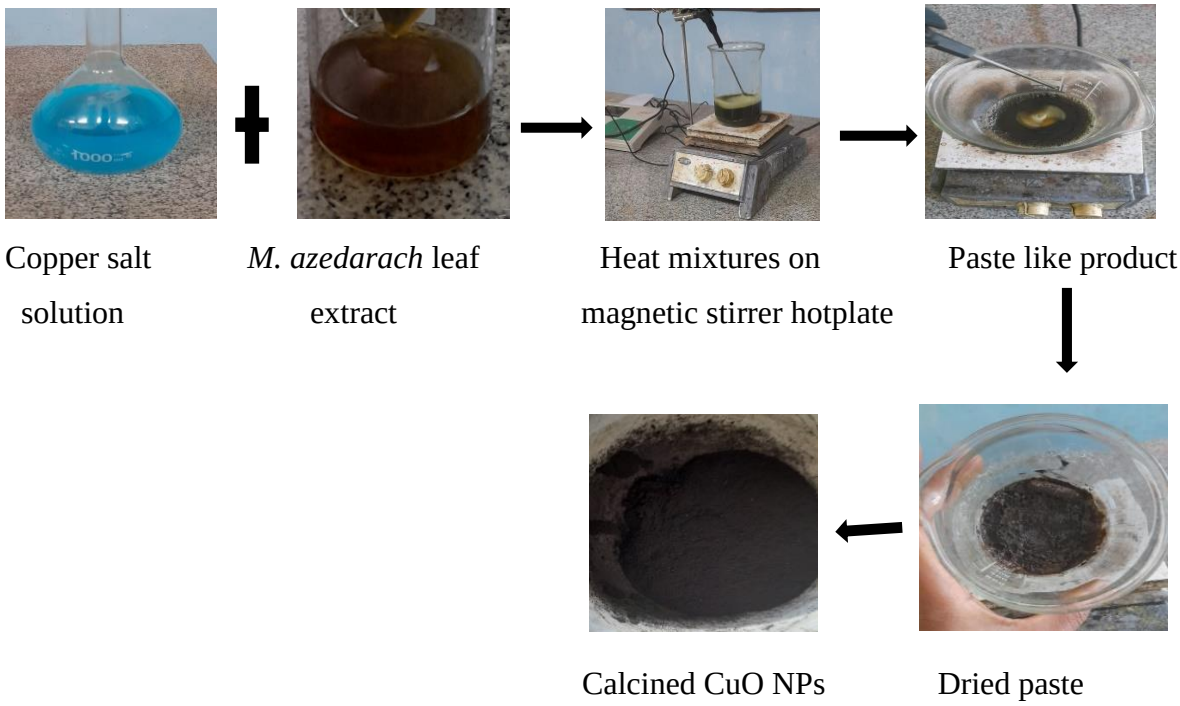

Figure: **8** Flow chart for synthesis of CuO nanoparticles by using *Melia azedarach leaf* extract.

3.3.3. Synthesis of Polyaniline (PANI)

Synthesis of PANI was based on mixing aqueous solution of aniline hydrochloride and APS (oxidizing agent used to imitate polymerization) at room temperature, followed by the separation of PANI hydrochloride precipitate by filtration and drying adopted from the literature [89] with little modification. 100 mL of 1 M aqueous HCl use (dopant used for formation of conductive salt) solution was mixed with 0.5 mL of aniline in a round-bottom flask and stirred for 1/2 hr. Then 5.71 g of ammonium persulfate was dissolved in 50 mL of distilled water and kept for 1 hr each separately. After that the two solutions was mixed and stirred by magnetic stirrer at room temperature until dark green precipitate (emerldine salt) was formed and waited for 4 hr to polymerize. Finally the precipitate was filtered and washed with 0.2 M HCl solution until the filtrate becomes clear, then with ethanol to remove the monomer and oligomer and with distilled water to

remove the remaining acid. Finally, the PANI precipitate was dried in an oven at 60 °C for 24 hr to obtain PANI powder.

3.3.4. Biosynthesis of CuO based Polyaniline Composites

A typical in-situ oxidative polymerization process was used to synthesis CuO based polyaniline composite using HCl and ammonium persulphate following literature [68] with little modifications. Briefly 0.5 mL of aniline monomer was dissolved in 100 mL of 1M HCl in a round-bottom flask. Next 0.9 g of CuO NPs was weighed and added in aniline hydrochloride solution and stirred the solution in an ice bath for 1/2 hr. Then 50 mL of 0.2 M ammonium persulphate solution was dropwise added to the solution and stirred at room temperature. The solution was further stirred for 5 hr using magnetic stirrer to complete the polymerization process. The mixture color was changed with formation of precipitate. The precipitate was collected by filter paper and washed with 0.2 M of HCl solution until the filtrate becomes clear, then with ethanol to remove the monomer and oligomer as well as with distilled water to remove the remaining acid. Finally the obtained product was dried in an oven at 80 ^{0}C for 24 hr to give CuO/PANI nanocomposites. Figure 9 shows flow chart for preparations of CuO/PANI NCs.

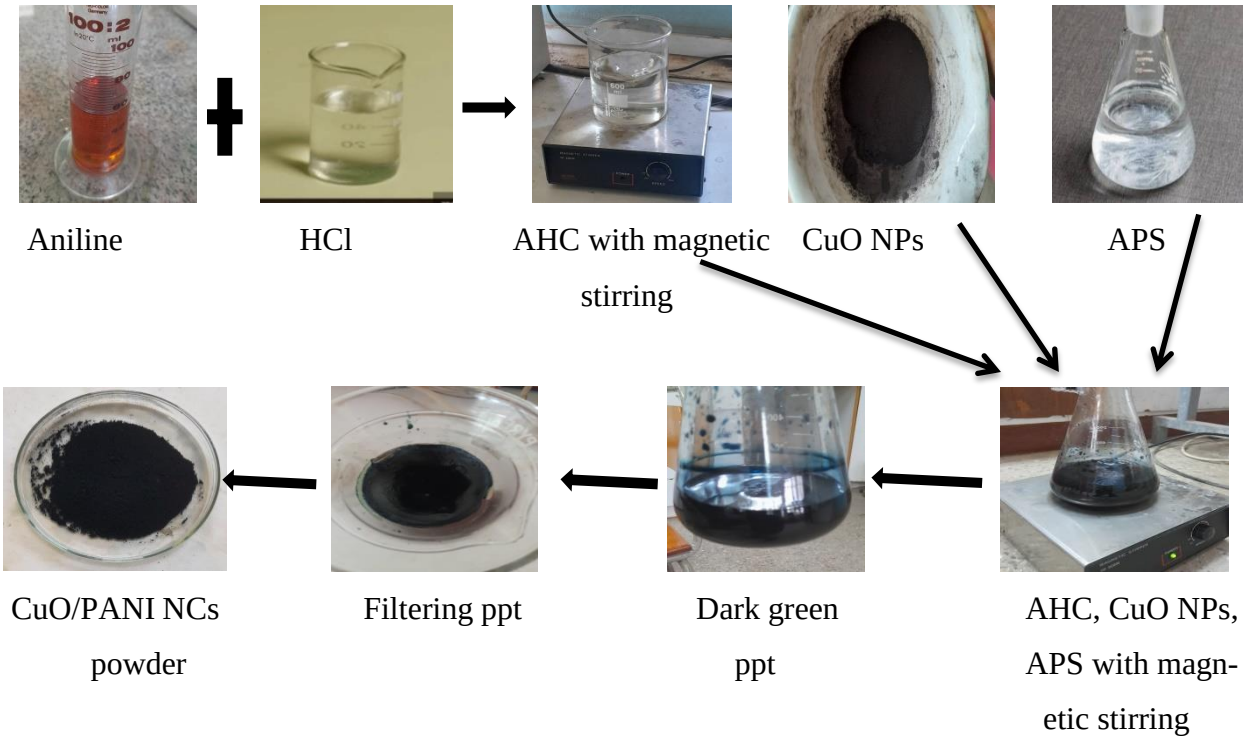

Figure: **9** Flow chart for preparations of CuO/PANI nanocomposite.

3.3.5. Anode Electrode Modification

Nanocatalyst was coated on PGE with HB pencil grade. Before coating four equal HB PGE was handmade with pencil lead having a diameter of 0.2 cm with 1 cm in length. Then it was soaked in distilled water for 24 hr and rinsed with phosphate buffer solution (PBS) at the time of setting up the MFC adopted from literature [90]. Next, the synthesized CuO NPs, PANI, and CuO/PANI nanocatalysts and polyvinyl alcohol (PVOH, MW = 44.05 g mol^{-1}) polymer binder solution was prepared. Polymer binder is used for increasing bonding force between nanocatalyst and bare PGE. A required amount of NPs and deionized water was mixed. Then PVOH was dissolved in 10 mL deionized water in the ratio of 1**:**5 (PVOH to NPs wt/wt %) and, mixing with NPs solution with magnetic stirring for 1 hr. Before coating on PGE surface, the mixture was kept for sonication to make uniform distribution of nanocatalyst throughout the solution. Then, a 100 μL of uniformly distributed nanocatalyst-based PVOH solution was coated on PGE surface by drop-cast method with the help of microsyringe adopted from [91] and finally it was dried for 12 hr at 60 °C using oven drying to improve its interface stability and bonding forces of the modified layer.

3.4. Nanocatalyst Characterizations

3.4.1. UV- Visible Spectrophotometric Analysis

The maximum wavelength and absorption spectrum of synthesized CuO NPs, PANI, and CuO/PANI nanocomposite was observed by using UV- Visible (Azzota SM-1600 SPECTRO-PHOTOMETER, USA) spectrometer in a wavelength range 200nm-800nm.

3.4.2. Fourier Transforms Infrared (FTIR) Spectra Analysis

The intermolecular bonding vibration, stretching motion and the existence of functional groups of all samples was performed by using Fourier transforms infrared (FTIR, Perkin Elmer 65, PerkinElmer, Inc., Waltham, USA) spectra in the range 4000–400 cm^{-1} with samples prepared using KBr pellets.

3.4.3. X- Ray Diffraction Analysis

The crystalline structural of CuO NPs, PANI, and CuO/PANI nanocomposite was examined with powder X-ray diffractometer (XRD-7000, Shimadzu, Japan) with a voltage of 40 kV and a current of 30 mA using a Cu Kα X-ray radiation source (1.5406 Å) in the 2θ range of 10°-80°.

3.4.4. Scanning Electron Microscopy (SEM) Analysis

Scanning electron microscopy (SEM) was performed using a JEOL Ltd. instrument with a model of JCM-6000Plus to elucidate structural morphology of CuO NPs, PANI, and CuO/PANI nano-composite.

3.5. Microbial Fuel Cell Setup and Operation

Single chamber microbial fuel cell was designed by using pencil graphite electrode (1 cm length, 0.2 cm diameter) both as anode and cathode electrodes. Four plastic containers were used to design four different MFCs. This MFC was assigned as MFC1, MFC2, MFC3 and MFC4 with bare PGE, CuO/PGE, PANI/PGE, and CuO/PANI/PGE anode electrode respectively and bare PGE cathode electrode for all devices. The anodic side was kept airtight and filled completely with 166 mg L^{-1} glucose substrate as a carbon source and wastewater sludge was added to achieve anaerobic experimental conditions while cathode side was exposed to air. Copper wire was used as external circuit to transfer electron from anode to cathode and voltage output was measured by digital multimeter (DMM, Model: mY-63).

3.5.1. Electrochemical Calculation

Open circuit voltage (OCV) was recorded continuously using a digital multi-meter (DMM, Model: mY-63) which directly connected between anode and cathode of MFC for 3 h/day after 10 min. stabilization for every 10 min interval. The polarization determination was monitored from closed circuit voltage (CCV) against external resistors for 4 continuous day within 30-minute time interval for 3 hr using Decade Resistance Box (ANSHUMAN, Model: DRB-7T) by varying an external resistance from 50 kΩ to 100 Ω. The current flow across each resistor was calculated from Ohm's law: $I = V/R$ and $P = V*I$, where P is power, I is current, and V is voltage. Similarly, the current density (J) was calculated from the ratio of current to surface area (A) of anode electrode (surface area for PGE was calculated by using ($2\pi rh + 2\pi r^2$) formula) and power density (PD) was calculated from multiplication of voltage and current density ($PD = V* J$).

4. RESULTS AND DISCUSSION

4.1. Characterization

4.1.1. UV-visible Analysis

The UV–visible absorption spectra of the CuO NPs, PANI, and CuO/PANI nanocomposite were investigated using UV-VIS spectroscopy and their spectrum has been depicted in Figure 10. The *Melia azedarach* leaf extract shows absorption peaks at 269 nm Figure 10 (black line) which indicates the existence of phytochemicals that essential for formations of CuO NPs include, flavonoids, tannins, phenolic acid, carbohydrate and terpenoids [87]. The peak at 210 nm and 323 nm shows conjugate system of carbonyl group. For copper oxide nanoparticles a maximum absorption peak is in the range of 200–350 nm [92]. As shown in Figure10 (red line) the maximum absorption peak of the synthesized CuO Nps observed at 253 nm. This maximum absorption transitions is charge transfer transitions from oxygen 2p orbitals to the copper 3d orbitals (ligand-to-metal charge transfer or vice versa. Synthesized PANI shows two characteristic absorption peaks between 315-342 nm (π-π* transition of the benzenoid rings) and 405-442 nm (π - polaron transition) [89]. So, in Figure 10 (blue line) the maximum absorption peak at 317 nm attributed to π-π* transition of C=C in benzenoid rings and the absorption spectra near 420 which formed in the range of 400-450 nm, are the characteristic transitions of π - polaron of PANI. In Figure10 (green line) two absorption peaks are observed with some shift to higher wave length from peak observed in CuO NPs and PANI spectra. The peak at 260 nm indicate absorption spectra of copper oxide nanoparticles while peak at 324 nm is π-π* transition of the benzenoid rings of polyaniline. The absence of an absorption band in the range of 400-445 nm and red shifted in the UV region with a more intense and broad peak than pure biosynthesized CuO Nps and PANI indicate the successful incorporation of CuO Nps in the PANI conducting matrix during in-situ polymerization to form CuO/PANI nanocomposite.

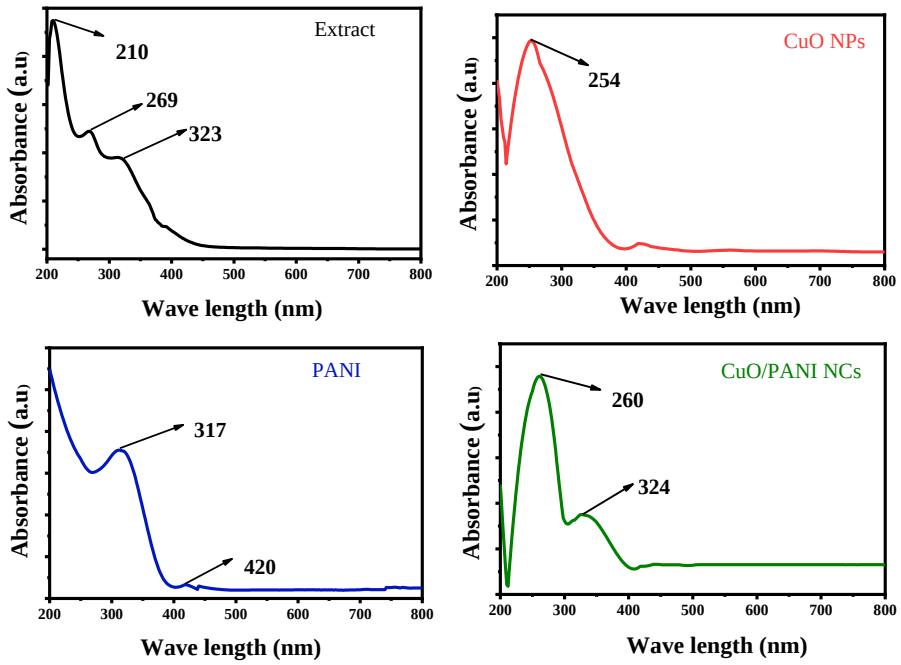

Figure: **10** UV-Vis absorption spectra of leaf extract (black line), CuO Nps (red line), PANI (blue line) and CuO/PANI NCs (green line).

4.1.1.1. Band gap of synthesized nanomaterials

The optical properties of synthesized nanoparticles are influenced by their electronic characteristics and band gap. Band gap is a minimum amount of energy required for electron to be excited from top of valance bond to the bottom of conduction band. It can be estimated by using UV-visible spectroscopy and Tauc's relation [93] . The general equation for Tauc's relations given by equation h;

$$(\alpha h\upsilon)^{1/n} = k(h\upsilon - E_g) \qquad (h)$$

Where, α is absorption coefficient, hυ is incident photon energy, k is constant, E_g is the band gap energy, n is the nature of transition that have a value of 1 for direct allowed band gap and 4 for indirect allowed band gap [94]. Therefore, Tauc's relation of equation (1) written as,

$$(\alpha h\upsilon)^2 = k(h\upsilon - E_g), \text{ for } n = 1(\text{direct band gap}). \qquad (i)$$

$$(\alpha h\upsilon)^{1/2} = k(h\upsilon - E_g), \text{ for } n = 4(\text{indirect band gap}) \qquad (j)$$

Also the band gap energy (E_g) of the materials can be calculated by using the following formula

$$E_g\,(eV) = 1240/\lambda(nm \qquad (k)$$

Where E_g is band gap energy in electron volt, λ is wavelength (nm) corresponds to absorption edge. The band gap was determined from the $(\alpha h\upsilon)^2$ Vs hυ curve by drawing an extrapolation of the data point to the photon energy axis where $(\alpha h\upsilon)^2 = 0$. The point where it touches the x- axis, at y = 0 is the band gap of material. Figure 11 shows the band gap for synthesized CuO NPs, PANI and CuO/PANI NCs with a value of n = 4 which is indirect band gap. The E_g of CuO NPs in this study Figure 11 (red line) was found to be 3.2 eV which have good agreement with previously reported work [95][96]. The band gap previously reported for bulk CuO could be between (1.9- 2.1). The higher band gap energy obtained in this study than reported is due to the quantum confinement effect, that means E_g value increase with a reduction in particle size [96][97]. The PANI could have two band gap of value 2.2 & 2.8 eV Figure 11(blue line), this band gap value is closely agree with previous reported work [98]. The band gap energy for synthesized nanocomposite was found to be 1.6 eV Figure 11(green line). This band gap energy is lower than pure CuO NPs and PANI due to larger size of nanocomposite during surface modifications. The lower band gap of nanocomposite indicates higher conductive properties of the synthesized nanocomposite which is the essential properties for better performance of microbial fuel cell.

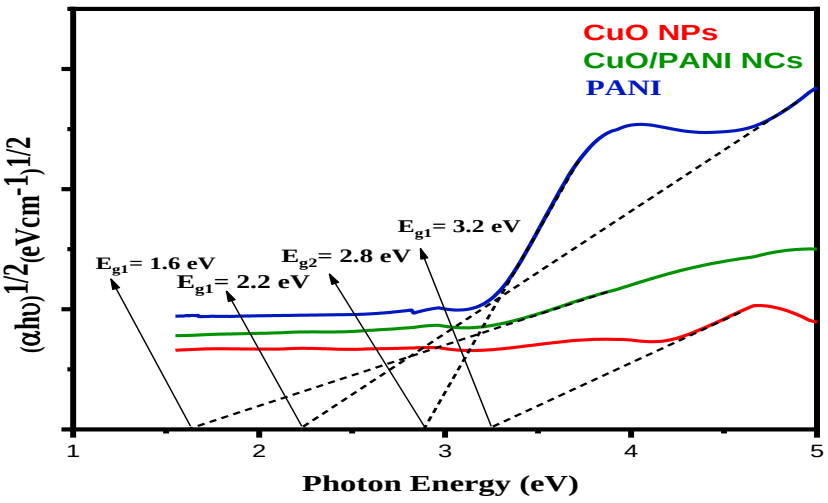

Figure: **11** Tauc's plot of CuO NPs, PANI and CuO/PANI nanocomposites.

4.1.2. FT-IR Analysis

Functional groups of synthesized sample were identified form Fourier transform infrared (FTIR) spectra, as shown in Figure 12. For *M. azedarach* leaf extract Figure 12 (black line) the peak observed at 3297 cm^{-1}, confirms the presence of OH stretching. This hydroxyl group indicates the presence of biomolecules such as, flavonoids, polyphenols, and alcohol functional group with different hydrogen bonds in extracts that used as reducing and capping agent for CuO NP synthesis. The peak at 2925 cm^{-1} confirms C-H stretching of alkane and the peak at 1656 cm^{-1} confirms C = O stretching of ketones, carboxylic acid, aldehydes, saturated aliphates and a stretch of α, β unsaturated esters. The peak at 1091 cm^{-1} indicates the presence of the C–N stretching vibrations of aliphatic amines. The observed peaks are closely agree with previous reported work [99]. Figure 12 (red line) show peaks associated with biosynthesized CuO NPs. The broad characteristic peak observed at 3373 cm^{-1} indicates asymmetric stretching vibrations of OH of phenolic compounds present in plant leaf extract. The absorption peak at 1634 cm^{-1} demonstrate C = O stretching of ketones, carboxylic acid, aldehydes, saturated aliphates and a stretch of α, β unsaturated esters. The peak at 1128 cm^{-1} corresponds to C-N stretching vibrations of aliphatic amines and the pure formation of CuO NPs confirms at narrow band 610 cm^{-1}. The confirmed peaks are closely related with previous report [100]. Figure12 (blue line) depicts the characteristic peak of polyaniline. The peak at 3442 cm^{-1} indicates the existence of N-H stretching. The peak at 1637 cm^{-1}, 1508 cm^{-1} and 823 cm^{-1} represents the C=N stretching vibrations of quinoid ring, C=C stretching vibrations benzenoid ring and out-of-plane bending of C-H respectively. So, the observed peaks form FT-IR analysis indicate the successfully formation of PANI which have close agreement with previously reported study [101][102]. When CuO is coated with PANI, associated peak of the CuO and PANI were observed with some sifting to higher wavelength, which indicate strong binding between the PANI and the nanoparticles [98]. In Figure 12 (green line) the peak at 3421 cm^{-1} indicates the existence of N-H stretching. The peak at 1579 cm^{-1}, 1493 cm^{-1}, 1120 cm^{-1}, and 539 cm^{-1} attributed C=N stretching vibrations of quinoid ring, C=C stretching vibrations benzenoid ring, C-N stretching vibrations of aliphatic amines and Cu–O bond formation respectively. From FT-IR spectra of CuO/PANI NCs the observed peak indicates the successful formations of desired nanocomposites.

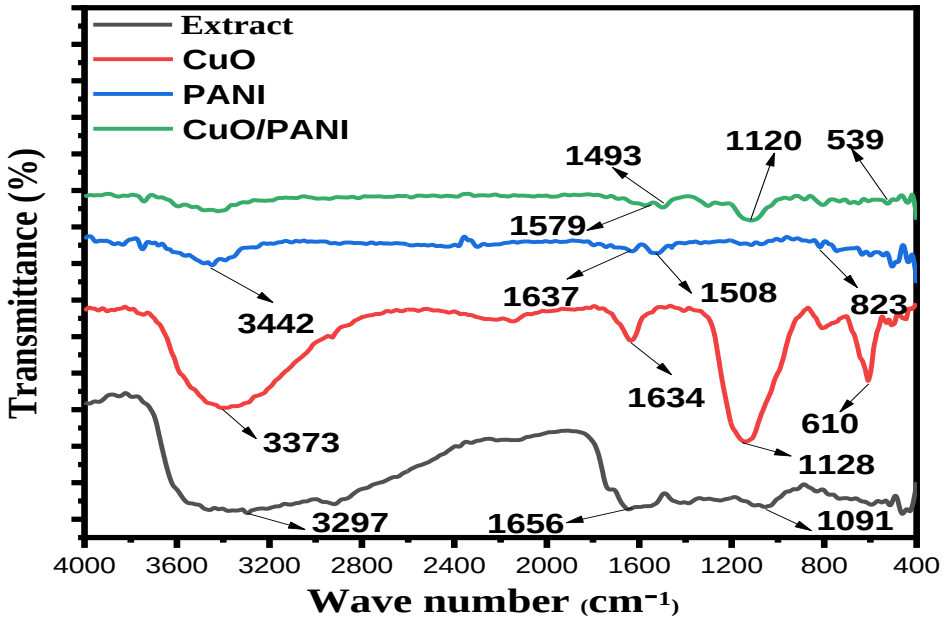

Figure: **12** FT-IR spectra of *Melia azedarach* leaf extract, CuO Nps, PANI and CuO/PANI nano-composites.

4.1.3. Scanning electron microscopy (SEM) analysis

The surface morphologies of CuO nanoparticle, PANI, and CuO/PANI nanocomposite have been investigated using scanning electron microscopy (SEM), and shown in Figure 13. Figure 13a depicts the surface morphologies of green synthesized CuO NPs. The image shows that the particle have some rough surface and other highly agglomerated spherical particle that are oriented randomly [88]. The formation of PANI morphology is determined by the synthesis conditions. The granular morphology of PANI powders is most common in PANI prepared by oxidative polymerization [101]. Figure 13b shows the amorphous structure of PANI with smooth surface, agglomerated, non-uniform, rough, irregular shape, and densely packed microstructures. The less-defined structures observed could be attributed to the utilization of strong oxidants and high concentrations of aniline during the acidic PANI synthesis process, in conjugation with the intrinsic properties of polyaniline. The Figure 13c depicts the morphology of CuO/PANI composites. The successful formation of the PANI/ metal oxide nanocomposites can be attributed to ionic interaction between the PANI and the metal oxide nanoparticles. Successful formation of metal oxide/polymer based nanocomposites could have either π-π or electrovalent interaction

between the metal oxide and polymer [103]. Formation of CuO/ PANI NCs is due electrostatic interaction between PANI and surface charge on copper oxide nanoparticles. In Figure13c below thin layer of PANI coexists with smooth spherical solid blocks copper oxide nanoparticles that indicate successful formation of desired CuO/PANI nanocomposites. From SEM morphology coating PANI on copper oxide makes the particles high agglomerated than uncoating one with higher porosity and superior particle dispersion compared to pure CuO nanoparticles and PANI powder. The improved porosity and particle dispersion represent promising characteristics that have the potential to enhance the catalytic performance of the synthesized nanoparticles. The porous structure of PANI/CuO NCs offers a substantial surface area, which facilitates bacteria growth and the formation of active biofilms on the anode surface.

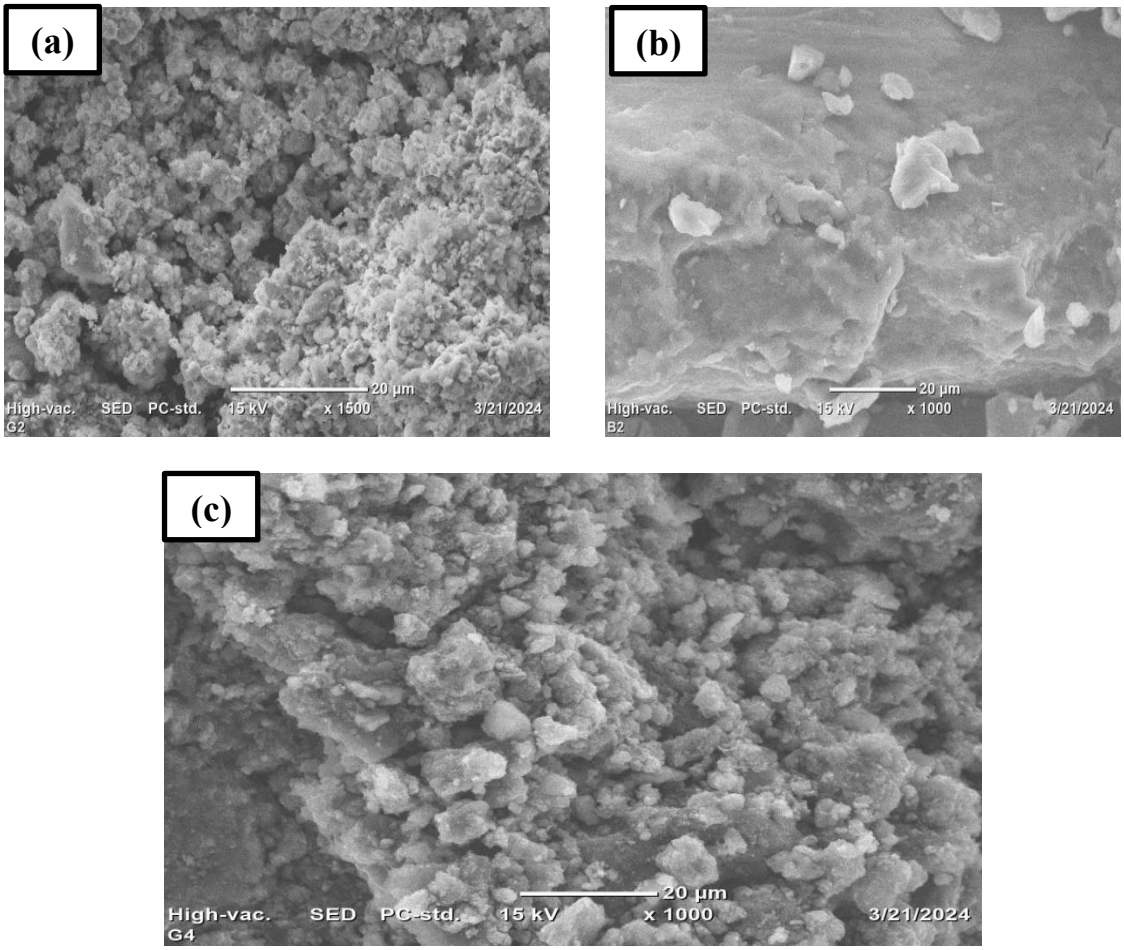

Figure: **13** SEM image of (a) CuO Nanoparticle (b) PANI and (c) CuO/PANI nanocomposites.

4.1.4. X-ray diffraction (XRD) analysis

The XRD pattern of CuO Nanoparticle, PANI and CuO/PANI nanocomposite are given in Figure 14 below. The XRD pattern of CuO Figure 14 (black line) shows a peak at 2θ of 32.55º, 35.57 º, 38.78º, 48.82º, 53.54º, 58.33 º, 61.59 º, 66.34 º, 72.48º, and 75.2º and corresponding (h k l) values (110), (002), (111), (202), (020), (202), (113), (022), (311) and (004) respectively which is agree with the previously reported work with JCPDS card No. 00-048–1548, [104][105]. The strong sharp peak indicates the high crystalline nature of CuO Nps. The XRD pattern of amorphous PANI Figure 14 (blue line) shows a broad peak at 2θ of 25.13 with corresponding (h k l) value (110). The XRD pattern of CuO/PANI nanocomposite Figure14 (green line) shows broad peak at 2θ of 25.19 with corresponding (h k l) value (110) which resembles pure PANI and peaks at 2θ of 35.58 and 38.79 with corresponding (h k l) value (110), (111) respectively could be resembles to CuO NPs. The slight shift of 2θ value in nanocomposite indicate the formation of CuO/PANI NCs from some interaction between PANI chain and CuO nanoparticles [68].the absence of other peak of CuO NPs in nanocomposites indicate the predominance of polyaniline on copper oxide nanoparticles.

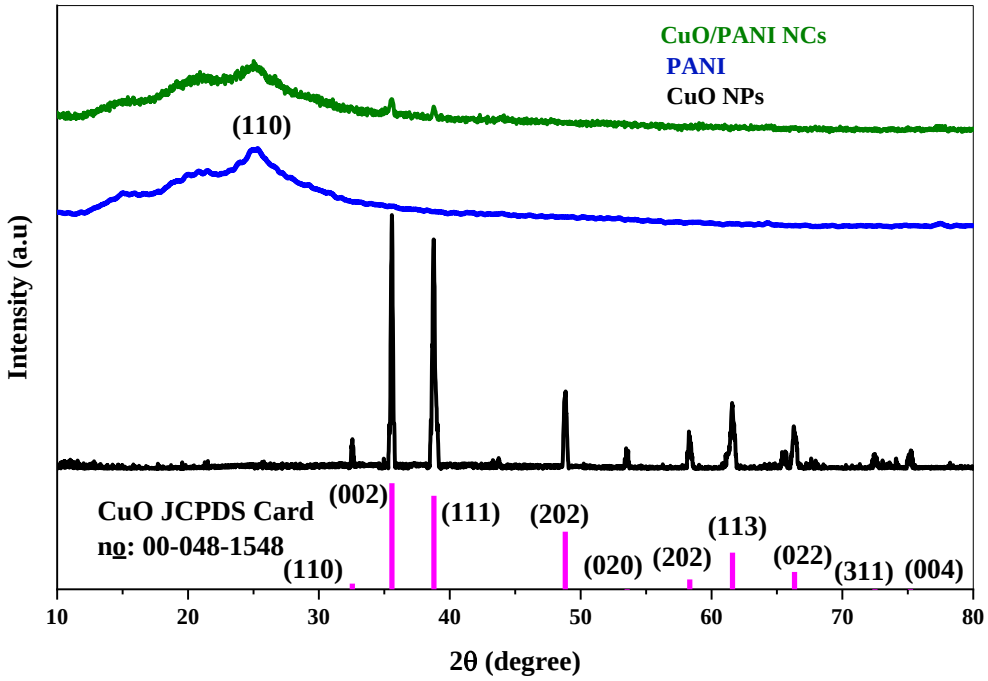

Figure: **14** XRD pattern of synthesized CuO Nps, PANI and CuO/PANI NCs.

4.1.4.1. Interplanar space (d) and Average crystalline size (D)

The estimations of the interplanar spacing in a lattice and the size of crystalline structures of synthesized material was calculated by using Braggs law and the Debye-Scherrer equation respectively [106].

$$n\lambda = 2d \sin\theta, \quad (3)$$

Whereas, d is interplanar space, n is an integer, λ is the XRD wavelength for Cu Kα (0.154 nm) and θ is the angle between the incident ray and the scattering planes.

$$D = k\lambda/\beta Cos\theta \quad (4)$$

Where, D is the average crystal size (nm), k is shape factor for an average crystallite (0.94), λ is the XRD wavelength (nm), β is the full width at half maximum (FWHM) of crystallite peak (measured in radians) and θ is Bragg's angle (°) of the XRD peak. Table 2 and 3 below shows the average crystal size and interplanar space of CuO NPs, PANI and CuO/PANI NCs respectively. The average crystalline size for CuO NPs, PANI and CuO/PANI could be 28.05, 3.2 and 20.6 nm respectively.

Table 2 XRD data used for calculation of interlayer spacing, crystalline size of CuO Nanoparticle.

No.	2θ (°)	d-spacing (nm)	FWHM (°)	Miller indices (hkl)	Crystallite size (nm)
1	32.55	0.0211	0.1702	110	45.7
2	35.57	0.0229	0.2307	002	33.4
3	38.78	0.0249	0.2924	111	26.1
4	48.82	0.0311	0.2415	202	30.5
5	53.54	0.0339	0.2116	020	34.1
6	58.33	0.0366	0.2675	202	26.4
7	61.59	0.0385	0.3668	113	18.9

8	66.34	0.0411	0.3357	022	20.2
9	72.48	0.0444	0.2579	311	25.3
10	75.2	0.0459	0.3285	004	19.5
					Average crystalline size = 28.05

Table 3 XRD data used for calculation of interlayer spacing, crystalline size of PANI and CuO/PANI nanocomposite.

No.	2θ (°)	d-spacing (nm)	FWHM (°)	Miller indices (hkl)	Crystallite size (nm)
PANI					
1	25.13	0.352	2.47501	110	3.2
CuO/PANI nanocomposite					
2	25.19	0.353	2.20841	110	3.5
3	35.56	0.0230	0.30632	110	25.19
4	38.79	0.0250	0.23158	111	33
					Average crystalline size = 20.5

4.2. Microbial fuel cell activity test

4.2.1. Electricity generation

An Open circuit voltage is one of the most crucial parameters to evaluate the catalytic activity of the prepared nanomaterial for improving the overall performance of microbial fuel cell. The

OCV output obtained by CuO, PANI, and CuO/PANI NCs modified PGE and bare PGE were operated for four continuous days. A continuous 180 minute measurement per day are shown in Figure15a.The highest mean open-circuit voltage (OCV) of 229 ± 11.3 mV (day 4), 315 ± 35.3 mV (day 2), 485 ± 15.5 mV (day 3) and 630 ± 10.6 mV (day 2) was produced by bare PGE, CuO/PGE, PANI/PGE and CuO/PANI/PGE respectively .From these four days continuous operation the second day was the better time to perform MFC using CuO/PANI/PGE than unmodified PGE. The highest OCV investigation throughout the day using CuO/PANI NCs binary composite-modified PGE was due to the strong cohesion between the bacteria and the CuO/PANI NCs catalyst to form conductive biofilm Figure15 b increase active surface area of electrode, this leading to improve fast electron transfer rates in MFC operation. Open circuit voltage (OCV) values generated by four electrodes for each day are given in Table 4. Based on these consistent OCV results, the prepared nanomaterial is considered as an effective catalyst to increase MFC performances under steady-state conditions.

Table 4 OCV output obtained using bare PGE, CuO/PGE, PANI/PGE and CuO/PANI/PGE modified PGE anode materials.

Time of operation	Electrode	Mean ± SD (mV)	Minimum (mV)	Maximum (mV)
1st day	PGE	177 ± 34.3	130	235
	CuO/PGE	269 ± 68.1	146	384
	PANI/PGE	460 ± 42.9	358	546
	CuO/PANI/PGE	532 ± 58.7	498	581
2nd day	PGE	202 ± 38.2	140	259
	CuO/PGE	315 ± 35.3	279	433
	PANI/PGE	457 ± 37.8	360	568
	CuO/PANI/PGE	630 ± 10.6	579	707

	PGE	227 ± 28.5	186	302
3rd day	CuO/PGE	290 ± 73.1	261	364
	PANI/PGE	485 ± 15.5	366	600
	CuO/PANI/PGE	576± 63.2	540	630
	PGE	229 ± 11.3	210	264
4th day	CuO/PGE	294 ± 74.1	252	354
	PANI/PGE	421 ± 24.5	330	530
	CuO/PANI/PGE	559 ± 67.2	522	615

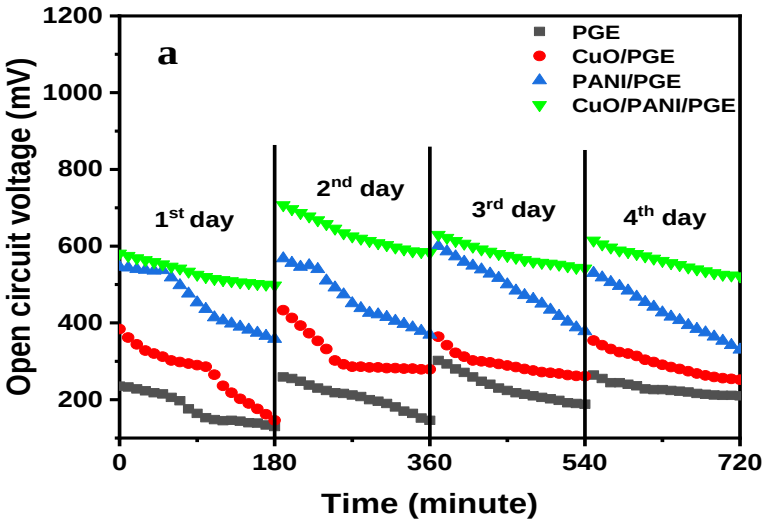

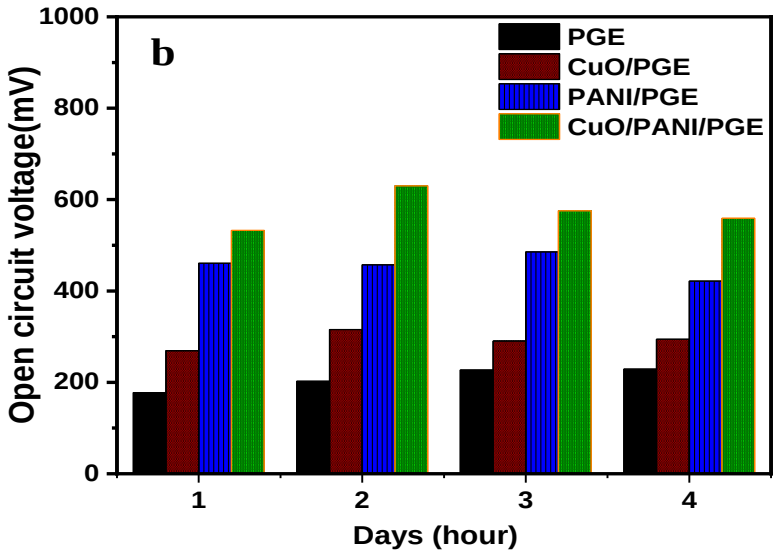

Figure: **15** Open-circuit voltage (a) and average open-circuit voltage (b) as a function of time for bare PGE, CuO/PGE, PANI/PGE and CuO/PANI/PGE.

4.2.2. Polarization curve

The polarization curve is a most important parameter in characterizing the performance of a microbial fuel cell (MFC). These plots demonstrate how well the MFC maintains its electric potential as a function of current density. The polarization curves of bare PGE, CuO/PGE, PANI/PGE, CuO/PANI/PGE hybrid composite towards MFC performance given in Figure 16, depicts three distinct regions: Frist region at high resistances and low current density there is a sudden potential drop. This potential drop is primarily due to activation losses, which are associated with the kinetic limitations of the electrochemical reactions occurring at the electrode- electrolyte interface. During migration of electrons from bacteria to anode surface, direct or indirect energy losses in the form of heat for initiations of redox reaction and bacteria metabolism (bacteria's require energy to undergo its metabolic activity).The second, region of constant and linear drop of electric potential at intermediate current density. This region represents ohmic losses, which means the potential drop is due to resistance of ion travels inside the leachate and interconnection between two electrodes. The third region shows rapid potential drop at low value of resistance and high current density. This region represents concentration losses, where the potential drop is due to depletion of reactants towards electrodes and limitations of product out of elec-

trode. The voltage value, 262 mV, 371 mV, 443 mV and 451mV represent open circuit voltage for MFC1, MFC2, MFC3, and MFC4 respectively and are achieved at infinite resistance. The four polarization curve of MFC1, MFC2, MFC3, and MFC4 show a sudden voltage drop to 230 mV, 349 mV, 406 mV and 399mV with corresponding current density of 66.34 $mAcm^{-2}$, 78.02 $mAcm^{-2}$, 128.2 $mAcm^{-2}$ and 140.6 $mAcm^{-2}$ respectively. The three potential drops should be limited by using diverse bacteria at the anode, reducing space between electrodes and increasing the ionic conductivity of the electrolyte and supplying new engineered bacteria which might have better metabolism.

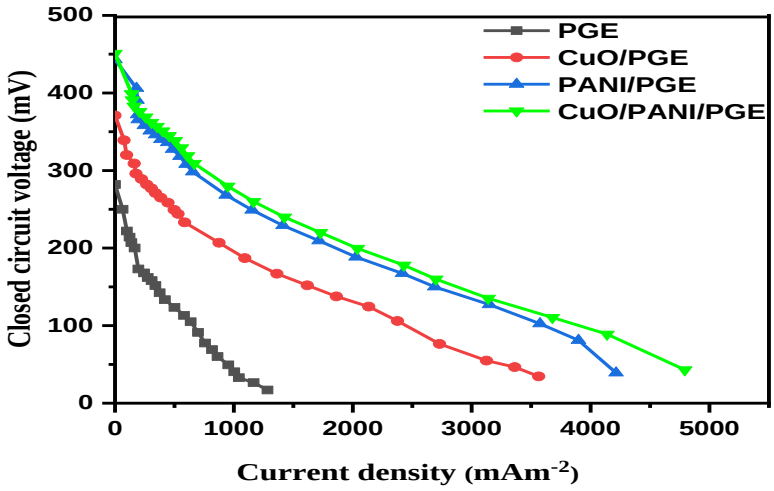

Figure: **16** Polarization curves of PGE, CuO/PGE, PANI/PGE, and CuO/PANI/PGE.

4.2.3. Power density curve

Power density curve is an important parameter used to characterize the performance of MFC. Its curve represents the power density as a function of current density. The electrocatalytic activity of CuO, PANI, and CuO/PANI hybrid composite modified PGE towards MFC performances were shown in Figure 17. Bare PGE exhibited the maximum power density of 65.67 mWm^{-2} with corresponding current densities of 580.21 mAm^{-2}, which has the lowest values due to the inefficient electrical conductivity. CuO/PGE exhibited the maximum power density of 265.75 mWm^{-2} at current density of 2134.34 mA m^{-2}, which shows the better performances than bare PGE due to its high electrical conductivity properties that lead to motivate a fast electron transfer rate between bacterial colonies and the electrode surface. PANI/PGE also shows higher power density of a value 387.91 mWm^{-2} with corresponding current density of 2418.06 mAm^{-2}. The

power density generated by PANI/PGE is also much higher in magnitude than bare PGE and CuO/PGE but is closer in power density with CuO/PANI/PGE at higher load resistance region. This might be occur when a peptide bond formed between bacteria and PGE surface which serve as a road to transfer electron rate effectively [13]. The maximum power density of 416.01 mWm^{-2} was produced by CuO/PANI/PGE. The current density formed at this maximum power density was 2429.56 mAm^{-2}. This power and current density of composite-modified PGE electrodes was 6.3 and 4 fold than unmodified PGE. This further improvement in performance is due to fulfillment of properties for better anode material such as (high electrical conductivity, stability, high porosity and etc.) of CuO coated with PANI which increase surface area of electrode by lowering the internal resistance found on it and facilitated the electron transfer between bacteria and electrode. A maximum power density is a point at which both internal and external resistances are equal. The resistances at this point have value 2817 Ω, 1072 Ω, 879 Ω and 941 Ω for bare PGE, CuO/PGE, PANI/PGE and CuO/PANI/PGE respectively.

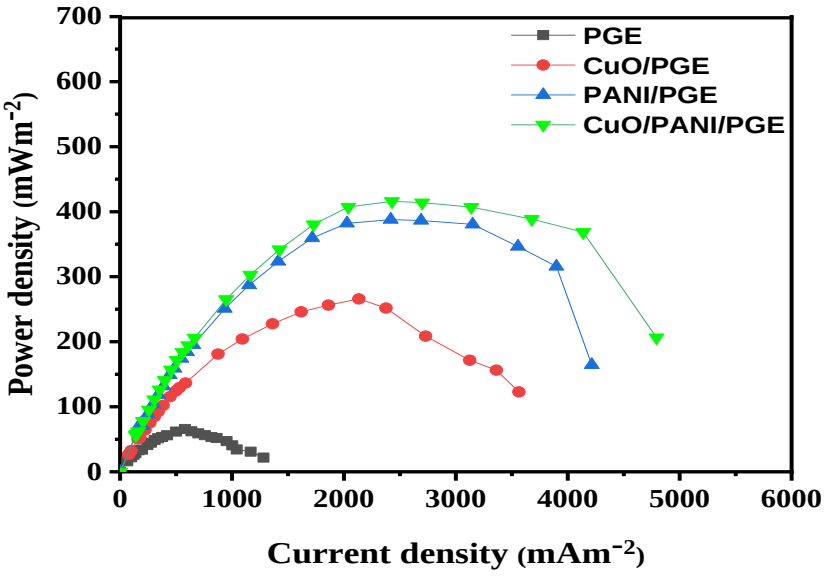

Figure: **17** power density curves of PGE, CuO/PGE, PANI/PGE, and CuO/PANI/PGE.

Table 5 Comparison of unmodified PGE, CuO/PGE, PANI/PGE and CuO/PANI/PGE with other literature.

Substrate (Fuel)	anode material	cathode material	OCV (mV)	PD_{max} (mW m^{-2})	J (mA m^{-2})	References
Acetate	PPy@MnO_2-CC	CC	660	2139.7 ± 67.5	5.25 ± 0.31	[46]
Glucose	α-MnO_2/PANI/PGE	PGE	650.61	426.26 ± 38.89	2485.51 ± 397.3	[13]
Glucose	MoO_2/PANI/CC	CC	700	1101	3000	[21]
Glucose	α-MnO_2/PANI/NiO / PGE	PGE	616.72	506.96	2545	[20]
Acetate	NiO/MnO /CF	CF	652	682	-	[107]
Acetate	PANI/rGO/CC	CF	-	1390	2670	[108]
Acetate	PANI/CF	CF	-	216	3300	[109]
Glucose	PGE	PGE	229	65.67	580.21	[This work]
Glucose	CuO/PGE	PGE	315	265.75	2134.34	[This work]
Glucose	PANI/PGE	PGE	485	387.91	2418.0	[This work]
Glucose	CuO/PANI/PGE	PGE	630	416.01	2429.56	[This work]

CC = Carbon cloth CF = carbon felt PGE = pencil graphite electrode

5. CONCLUSION AND RECOMMENDATION

5.1. Conclusion

Performance of microbial fuel cell can be improved by modifying its electrodes with different nanomaterials. In this study CuO nanoparticles PANI, and CuO/PANI NCs was prepared by, green method using *Melia azedarach* leaf extract, oxidative polymerization method, and dispersing biosynthesized CuO NPs in the conductive PANI matrix using the in situ polymerization method. The synthesized samples were characterized by using UV-Visible, FT-IR, SEM and XRD. The findings obtained from this study are; the highest mean open circuit voltage (OCV) of a value 229 ± 11.3 mV, 315 ± 35.3 mV, 485 ± 15.5 mV, and 630 ± 10.6 mV was generated by bare PGE, CuO/PGE, PANI/PGE, CuO/PANI/PGE respectively. The maximum power density and related current densities obtained with bare PGE, CuO/PGE, and PANI/PGE was 265.75 mWm^{-2} & 2134.34 mA m^{-2}, 387.91 mWm^{-2} & 2418.06 mAm^{-2} and 65.67 mWm^{-2} & 580.21 mAm^{-2} respectively. The maximum power density and corresponding current density obtained with CuO/PANI/PGE was 416.01 mWm^{-2} and 2429.56 mAm^{-2} respectively. The prepared binary nanocomposite exhibit 6.3 and 4-fold higher in power and current densities respectively than unmodified PGE. The findings obtained from the study indicate that the synthesized CuO/PANI nanocomposites that modify PGE elucidate a better performance as compared to other. In generally modification of microbial fuel cell electrodes with low cost, and highly conductive nanomaterial is a better way to improve performance of the device.

5.2. Recommendation

The following recommendations were made for future researcher. For future study further characterization of the prepared sample by energy dispersive X-Ray (EDX) and Transition Electron Microscopy (TEM) is important in order to investigate the elemental distribution, particle size and more detail morphology of the synthesized samples. Again the electrocatalytic activities and impedance of prepared sample should be investigated from cyclic voltammetry and electrochemical impedance spectroscopy. The future study should be included characterization of the prepared sample with cyclic voltammetry and electrochemical impedance spectroscopy. Further improvements are required including alternative MFC configuration and electrode modification to improve power production. The future study should be constructed double chamber microbial

fuel cell to investigate the output from device and also use the prepared sample for cathode modification in order to compare the result with that obtained from anode modification. Again the ternary composite is considered as an effective catalyst to increase performance than binary composite. For further studies it is good idea to prepare different ternary composite catalyst for microbial fuel cell electrode modification.

REFERENCES

[1] K. Gengiah, G. L. P. Moses, and G. Baskar, 'Bioethanol production from *Codium tomentosum* residue', *Energy Sources Part Recovery Util. Environ. Eff.*, pp. 1–10, 2020, doi: 10.1080/15567036.2020.1771481.

[2] Y. Dessie, S. Tadesse, and R. Eswaramoorthy, 'Review on manganese oxide based biocatalyst in microbial fuel cell: Nanocomposite approach', *Mater. Sci. Energy Technol.*, vol. 3, pp. 136–149, 2020, doi: 10.1016/j.mset.2019.11.001.

[3] M. C. Potter, 'Electrical effects accompanying the decomposition of organic compounds', *Proc. R. Soc. Lond. Ser. B Contain. Pap. Biol. Character*, vol. 84, pp. 260–276, 1911.

[4] H. Roy, T. Ur. Rahman, N. Tasnim, J. Arju, Md. M. Rafid, Md. R. Islam, Md. N. Pervez, Y. Cai, V. Naddeo, and Md. Sh. Islam, 'Microbial fuel cell construction features and application for sustainable wastewater treatment', *Membranes.*, vol. 13, p. 490, 2023, doi: 10.3390/membranes13050490.

[5] D. Pant, G. Van Bogaert, L. Diels, and K. Vanbroekhoven, 'A review of the substrates used in microbial fuel cells (MFCs) for sustainable energy production', *Bioresour. Technol.*, vol. 101, pp. 1533–1543, 2010, doi: 10.1016/j.biortech.2009.10.017.

[6] J. Kariuki, E. Ervin, and C. Olafson, 'Development of a novel, low-cost, disposable wooden pencil graphite electrode for use in the determination of antioxidants and other biological Compounds', *Sensors*, vol. 15, pp. 18887–18900, 2015, doi: 10.3390/s150818887.

[7] I. G. David, D. E. Popa, and M. Buleandra, 'Pencil graphite electrodes: A versatile tool in electroanalysis', *J. Anal. Methods Chem.*, vol. 2017, pp. 1–22, 2017, doi: 10.1155/2017/1905968.

[8] R. Tsuji, H. Masutani, Y. Haruyama, M. Niibe, S. Suzuki, Sh. Honda, Y. Matsuo, A. Heya, N. Matsuo, and S. Ito, 'Water electrolysis using flame-annealed pencil graphite rods', *ACS Sustain. Chem. Eng.*, vol. 7, pp. 5681–5689, 2019, doi: 10.1021/acssuschemeng.8b04688

[9] Y. Qiao, X. S. Wu, and C. M. Li, 'Interfacial electron transfer of *Shewanella putrefaciens* enhanced by nanoflaky nickel oxide array in microbial fuel cells', *J. Power Sources.*, vol. 266, pp. 226–231, 2014, doi: 10.1016/j.jpowsour.2014.05.015.

[10] C. Santoro, S. Babanova, K. Artyushkova, J. A. Cornejo, L. Ista, O. Bretschger, E. Marsili, P. Atanassov, and A. J. Schuler, 'Influence of anode surface chemistry on microbial fuel cell

operation', *Bioelectrochemistry*, vol. 106, pp. 141–149, 2015, doi: 10.1016/j.bioelechem.2015.05.002.

[11] A. A. Yaqoob, M. N. M. Ibrahim, and S. Rodríguez-Couto, 'Development and modification of materials to build cost-effective anodes for microbial fuel cells (MFCs): An overview', *Biochem. Eng. J.*, vol. 164, p. 107779, 2020, doi: 10.1016/j.bej.2020.107779.

[12] X. Wan, Sh. Yang, Z. Cai, Q. He, Y. Ye, Y. Xia, G. Li, and J. Liu, 'Facile synthesis of MnO_2 nanoflowers/N-doped reduced graphene oxide composite and its application for simultaneous determination of dopamine and uric acid', *Nanomaterials.*, vol. 9, p. 847, 2019, doi: 10.3390/nano9060847.

[13] Y. Dessie, S. Tadesse, R. Eswaramoorthy, and Y. Adimasu, 'Biosynthesized α -MnO_2 -based polyaniline binary composite as efficient bioanode catalyst for high-performance microbial fuel cell', *Life*, vol. 14, pp. 541–568, 2021, doi: 10.1080/26895293.2021.1934123.

[14] S. Mathew and P. C. Thomas, 'Fabrication of polyaniline nanocomposites as electrode material for power generation in microbial fuel cells', *Mater. Today Proc.*, vol. 33, pp. 1415–1419, 2020, doi: 10.1016/j.matpr.2020.06.502.

[15] W. Chen, Z. Liu, G. Su, Y. Fu, X. Zai, Ch. Zhou, and J. Wang, 'Composite-modified anode by MnO_2 /polypyrrole in marine benthic microbial fuel cells and its electrochemical performance: Composite-modified anode by MnO2/polypyrrole', *Int. J. Energy Res.*, vol. 41, pp. 845–853, 2017, doi: 10.1002/er.3674.

[16] F. Nourbakhsh, M. Mohsennia, and M. Pazouki, 'Nickel oxide/carbon nanotube/polyaniline nanocomposite as bifunctional anode catalyst for high-performance *Shewanella*-based dual-chamber microbial fuel cell', *Bioprocess Biosyst. Eng.*, vol. 40, pp. 1669–1677, 2017, doi: 10.1007/s00449-017-1822-y.

[17] J. Singh, T. Dutta, K.-H. Kim, M. Rawat, P. Samddar, and P. Kumar, '"Green" synthesis of metals and their oxide nanoparticles: Applications for environmental remediation', *J. Nanobiotechnology.*, vol. 16, p. 84, 2018, doi: 10.1186/s12951-018-0408-4.

[18] M. Aminuzzaman, L. M. Kei, and W. H. Liang, 'Green synthesis of copper oxide (CuO) nanoparticles using banana peel extract and their photocatalytic activities', *AIP Conference Proceedings.*, p. 020016, 2017, doi: 10.1063/1.4979387.

[19] E. Dinga, A. Ekennia, C. U. Ogbonna, D. A. Udu, M. N. Mthiyane, U. Marume, and D. C. Onwudiwe, 'Phyto-mediated synthesis of MgO nanoparticles using *Melia azedarach* seed

extract: Larvicidal and antioxidant activities', *Sci. Afr.*, vol. 17, p. e01366, 2022, doi: 10.1016/j.sciaf.2022.e01366.

[20] Y. Dessie, S. Tadesse, and R. Eswaramoorthy, 'Surface roughness and electrochemical performance properties of biosynthesized α-MnO_2/NiO-based polyaniline ternary composites as efficient catalysts in microbial fuel cells', *J. Nanomater.*, vol. 2021, pp. 1–21, 2021, doi: 10.1155/2021/7475902.

[21] Geetanjali, R. Rani, and S. Kumar, 'High-capacity polyaniline-coated molybdenum oxide composite as an effective catalyst for enhancing the electrochemical performance of the microbial fuel cell', *Int. J. Hydrog. Energy*, vol. 44, pp. 16933–16943, 2019, doi: 10.1016/j.ijhydene.2019.04.201.

[22] Z. Lv, Y. Chen, H. Wei, F. Li, Y. Hu, Ch. Wei, and Ch. Feng, 'One-step electrosynthesis of polypyrrole/graphene oxide composites for microbial fuel cell application', *Electrochimica Acta.*, vol. 111, pp. 366–373, 2013, doi: 10.1016/j.electacta.2013.08.022.

[23] S. G. A. Flimban, I. M. I. Ismail, T. Kim, and S.E. Oh, 'Overview of Recent advancements in the microbial fuel cell from fundamentals to applications: Design, major elements, and scalability', *Energies.*, vol. 12, 2019, doi: 10.3390/en12173390.

[24] H. Gul, W. Raza, J. Lee, M. Azam, M. Ashraf, and K.-H. Kim, 'Progress in microbial fuel cell technology for wastewater treatment and energy harvesting', *Chemosphere.*, vol. 281, p. 130828, 2021, doi: 10.1016/j.chemosphere.2021.130828.

[25] T. Q. H. Kieu, T. Y. Nguyen, and C. L. Do, 'Effect of different catholytes on the removal of sulfate/sulfide and electricity generation in sulfide-oxidizing fuel cell', *Molecules.*, vol. 28, p. 6309, 2023, doi: 10.3390/molecules28176309.

[26] A. Naha, R. Debroy, D. Sharma, M. P. Shah, and S. Nath, 'Microbial fuel cell: A state-of-the-art and revolutionizing technology for efficient energy recovery', *Clean. Circ. Bioeconomy.*, vol. 5, p. 100050, 2023, doi: 10.1016/j.clcb.2023.100050.

[27] D. Das, Ed., 'Microbial fuel cell: A bioelectrochemical system that converts waste to watts', 2018, doi: 10.1007/978-3-319-66793-5.

[28] P. P. Włodarczyk and B. Włodarczyk, 'Wastewater treatment and electricity production in a microbial fuel cell with Cu–B alloy as the cathode catalyst', *Catalysts.*, vol. 9, 2019, doi: 10.3390/catal9070572.

[29] D. R. Bond and D. R. Lovley, 'Electricity production by *Geobacter sulfurreducens* attached to electrodes', *Appl. Environ. Microbiol.*, vol. 69, pp. 1548–1555, 2003, doi: 10.1128/AEM.69.3.1548-1555.2003.

[30] I. A. Ieropoulos, J. Greenman, C. Melhuish, and J. Hart, 'Comparative study of three types of microbial fuel cell', *Enzyme Microb. Technol.*, vol. 37, pp. 238–245, 2005, doi: 10.1016/j.enzmictec.2005.03.006.

[31] 'Types: Microbial fuel cells', 2023.

[32] S. C. Santra, S. C. Santra, S. Banerjee, S. Bharati, and A. Mallick, 'Microbial fuel cell', vol. 25, 2014.

[33] D. P. B. T. B. Strik, H. V. M. Hamelers (Bert), J. F. H. Snel, and C. J. N. Buisman, 'Green electricity production with living plants and bacteria in a fuel cell', *Int. J. Energy Res.*, vol. 32, pp. 870–876, 2008, doi: 10.1002/er.1397.

[34] Z. Du, H. Li, and T. Gu, 'A state of the art review on microbial fuel cells: A promising technology for wastewater treatment and bioenergy', *Biotechnol. Adv.*, vol. 25, pp. 464–82, 2007, doi: 10.1016/j.biotechadv.2007.05.004.

[35] A. R. P. Hidayat, A. R. Widyanto, A. Asranudin, R. Ediati, D. O. Sulistiono, H. S. Putro, D. Sugiarso, D. Prasetyoko, A. S. Purnomo, H. Bahruji, B. T. I. Ali, and I. Sh. Caralin, 'Recent development of double chamber microbial fuel cell for hexavalent chromium waste removal', *J. Environ. Chem. Eng.*, vol. 10, p. 07505, 2022, doi: 10.1016/j.jece.2022.107505.

[36] J. M. Monier, L. Niard, N. Haddour, B. Allard, and F. Buret, 'Microbial Fuel Cells: From biomass (waste) to electricity', *Melecon. Mediterranean Electrotechnical Conference.*, pp. 663–668, 2018, doi: 10.1109/Melcon.2018.4618511.

[37] A. Banerjee, R. K. Calay, and F. E. Eregno, 'Role and important properties of a membrane with its recent advancement in a microbial fuel cell', *Energies.*, vol. 15, 2022, doi: 10.3390/en15020444.

[38] S. Kalathil, S. Patil, and D. Pant, 'Microbial fuel cells: Electrode materials', in *Encyclopedia of Interfacial Chemistry.*, pp. 309-318, 2017. doi: 10.1016/B978-0-12-409547-2.13459-6.

[39] J. Wei, P. Liang, and X. Huang, 'Recent progress in electrodes for microbial fuel cells', *Bioresour. Technol.*, vol. 102, pp. 9335–9344, 2011, doi: 10.1016/j.biortech.2011.07.019.

[40] P. Mishra, S. P. Mishra, S. Datta, S. Taraphder, S. Panda, R. Saikhom, M. Laishram, D.P. Swain, and R.Y. Nanotkar, 'Microbial Fuel Cell (MFC): Recent advancement and its application', *Int. J. Pure Appl. Biosci.*, vol. 5, pp. 911–923, 2017, doi: 10.18782/2320-7051.2770.

[41] E. Y. Konovalova, D. I. Stom, G.O. Zhdanova, D. A. Yuriev, Y. Li, Dr. L. Barbora, and P. Goswami, 'The microorganisms used for working in microbial fuel cells', *International conference on electrical, electronics, materials and applied science.*, p. 020017, 2018, doi: 10.1063/1.5031979.

[42] H. J. Kim, H. S. Park, M. S. Hyun, I. S. Chang, M. Kim, and B. H. Kim, 'A mediatorless microbial fuel cell using a metal reducing bacterium, *Shewanella putrefaciens*', *Enzyme Microb. Technol.*, vol. 30, pp. 145–152, 2002, doi: 10.1016/S0141-0229(01)00478-1.

[43] M. Tong, S. Li, Z. Du, and H. Li, 'Enrichment of an electrochemically active bacterial community using microbial fuel cell', *Proceedings of ISES World Congress.*, pp. 2434–2438, 2018, doi: 10.1007/978-3-540-75997-3-493.

[44] J. V. Boas, V. B. Oliveira, M. Simões, and A. M. F. R. Pinto, 'Review on microbial fuel cells applications, developments and costs', *J. Environ. Manage.*, vol. 307, p. 114525, 2022, doi: 10.1016/j.jenvman.2022.114525.

[45] Q. Maqsood, E. Ameen, M. Mahnoor, A. Sumrin, M. W. Akhtar, R. Bhattacharya, and D. Bose, 'Applications of microbial fuel cell technology and strategies to boost bioreactor performance', *Nat. Environ. Pollut. Technol.*, vol. 21, pp. 1191–1199, 2022, doi: 10.46488/nept.2022.v21i03.024.

[46] X. Zhao, T. Tian, M. Guo, X. Liu, and X. Liu, 'Cauliflower-like polypyrrole@MnO_2 modified carbon cloth as a capacitive anode for high-performance microbial fuel cells', *J. Chem. Technol. Biotechnol.*, vol. 95, pp. 163–172, 2020, doi: 10.1002/jctb.6218.

[47] A. D. Juan, 'Microbial Fuel Cell: Literature review', 2014, doi: 10.13140/2.1.4481.0569.

[48] A. Saravanan, S. Karishma, P. S. Kumar, P. R. Yaashikaa, S. Jeevanantham, and B. Gayathri, 'Microbial electrolysis cells and microbial fuel cells for biohydrogen production: current advances and emerging challenges', *Biomass Convers. Biorefinery.*, vol. 13, pp. 8403–8423, 2023, doi: 10.1007/s13399-020-00973-x.

[49] H. Yang, M. Zhou, M. Liu, W. Yang, and T. Gu, 'Microbial fuel cells for biosensor applications', *Biotechnol. Lett.*, vol. 37, pp. 2357–2364, 2015, doi: 10.1007/s10529-015-1929-7.

[50] S. Li, C. Cheng, and A. Thomas, 'Carbon-based microbial fuel cell electrodes: From conductive supports to active catalysts', *Adv. Mater.*, vol. 29, p. 1602547, 2017, doi: 10.1002/adma.201602547.

[51] Y. Hindatu, M. S. M. Annuar, and A. M. Gumel, 'Mini review: Anode modification for improved performance of microbial fuel cell', *Renew. Sustain. Energy Rev.*, vol. 73, pp. 236–248, 2017, doi: 10.1016/j.rser.2017.01.138.

[52] S. Sukumar, A. Rudrasenan, and D. Padmanabhan Nambiar, 'Green synthesized rice-shaped copper oxide nanoparticles using *Caesalpinia bonducella* seed extract and their applications', *ACS Omega.*, vol. 5, pp. 1040–1051, 2020, doi: 10.1021/acsomega.9b02857.

[53] R. P. Allaker, 'Nanoparticles and the control of oral biofilms', *Nanobiomaterials in Clinical Dentistry.*, 2013, pp. 203–227. doi: 10.1016/B978-1-4557-3127-5.00010-6.

[54] S. M. Ambalagi, M. Devendrappa, S. Nagaraja, and B. Sannakki, 'Dielectric properties of PANI/CuO nanocomposites', *IOP Conf. Ser. Mater. Sci. Eng.*, vol. 310, p. 012081, 2018, doi: 10.1088/1757-899X/310/1/012081.

[55] M. Naseer, R. Ramadan, J. Xing, and N. A. Samak, 'Facile green synthesis of copper oxide nanoparticles for the eradication of multidrug resistant *Klebsiella pneumonia* and *Helicobacter* pylori biofilms', *Int. Biodeterior. Biodegrad.*, vol. 159, p. 105201, 2021, doi: 10.1016/j.ibiod.2021.105201.

[56] A. E. D. Mahmoud, K. M. Al-Qahtani, S. O. Alflaij, S. F. Al-Qahtani, and F. A. Alsamhan, 'Green copper oxide nanoparticles for lead, nickel, and cadmium removal from contaminated water', *Sci. Rep.*, vol. 11, p. 12547, 2021, doi: 10.1038/s41598-021-91093-7.

[57] D. M. Nzilu, E. S. Madivoli, D. S. Makhanu, S. I. Wanakai, G. K. Kiprono, and P. G. Kareru, 'Green synthesis of copper oxide nanoparticles and its efficiency in degradation of rifampicin antibiotic', *Sci. Rep.*, vol. 13, p. 14030, 2023, doi: 10.1038/s41598-023-41119-z.

[58] A. Bukhari, I. Ijaz, E. Gilani, A. Nazir, H. Zain, R. Saeed, S. S. Alarfaji, S. Hussain, R. Aftab, and Y. Naseer, 'Green synthesis of metal and metal oxide nanoparticles using different plants' parts for antimicrobial activity and anticancer activity: a Review Article', *Coatings.*, vol. 11, p. 1374, 2021, doi: 10.3390/coatings11111374.

[59] Y. Dessie and S. Admassie, ‘Electrochemical study of conducting polymer/lignin composites’, *Orient. J. Chem.*, vol. 29, pp. 1359–1369, 2013, doi: 10.13005/ojc/290411.

[60] S. Sharma, P. Sudhakara, A. A. B. Omran, J. Singh, and R. A. Ilyas, ‘Recent trends and developments in conducting polymer nanocomposites for multifunctional applications’, *Polymers.*, vol. 13, 2021, doi: 10.3390/polym13172898.

[61] E. Antolini, ‘Composite materials for polymer electrolyte membrane microbial fuel cells’, *Biosens. Bioelectron.*, vol. 69, pp. 54–70, 2015, doi: 10.1016/j.bios.2015.02.013.

[62] Y. Dessie and S. Tadesse, ‘A Review on advancements of nanocomposites as efficient anode modifier catalyst for microbial fuel cell performance improvement’, *J. Chem. Rev.*, vol. 3, 2021, doi: 10.22034/jcr.2021.314327.1128.

[63] L. I. Nadaf and K. S. Venkatesh, ‘Polyaniline-copper oxide nanocomposites: Synthesis and characterization’, *Mater. Sci. Res. India*, vol. 12, pp. 108–111, 2015, doi: 10.13005/msri/120204.

[64] P. H. C. Camargo, K. G. Satyanarayana, and F. Wypych, ‘Nanocomposites: Synthesis, structure, properties and new application opportunities’, *Mater. Res.*, vol. 12, pp. 1–39, 2009, doi: 10.1590/S1516-14392009000100002.

[65] D. M. Jundale, S. T. Navale, G. D. Khuspe, D. S. Dalavi, P. S. Patil, and V. B. Patil, ‘Polyaniline–CuO hybrid nanocomposites: Synthesis, structural, morphological, optical and electrical transport studies’, *J. Mater. Sci. Mater. Electron.*, vol. 24, pp. 3526–3535, 2013, doi: 10.1007/s10854-013-1280-5.

[66] D. R. S. Yadav, ‘Analytical study of polyaniline-copper (II) oxide nano composite by wet chemical route’, *Research in Chemistry*, vol. 2, pp. 86–92, 2021.

[67] N. Maruthi, M. Faisal, N. Raghavendra, B. P. Prasanna, S. R. Manohara, and M. Revanasiddappa, ‘Anticorrosive polyaniline-coated copper oxide (PANI/CuO) nanocomposites with tunable electrical properties for broadband electromagnetic interference shielding’, *Colloids Surf. Physicochem. Eng. Asp.*, vol. 621, p. 126611, 2021, doi: 10.1016/j.colsurfa.2021.126611.

[68] S. Vyas, A. Shukla, S. J. Shivhare, V. S. Bagal, and N. Upadhyay, ‘High performance conducting nanocomposites polyaniline (PANI)-CuO with enhanced antimicrobial activity for

biomedical applications', *ES Mater. Manuf.*, vol. 15, pp. 46-52, 2022, doi: 10.30919/esmm5f468.

[69] J. F. Sifuentes, K. V. S. Cardona, F. A. Arreazola, M. S. Domingues, L. L. G. Tovar, S. S. Guzman, N. F. G. M. D. Oca, N. A. G. Gomez, and E. M. Sanchez, 'Preparation of CuO/CNF composite and its performance as anode in a microbial fuel cell with Shewanella oneidensis in a half cell configuration', *J. Mater. Sci. Mater. Electron.*, vol. 29, pp. 15784–15794, 2018, doi: 10.1007/s10854-018-9307-6.

[70] F. Dong, P. Zhang, K. Li, X. Liu, and P. Zhang, 'Nano copper oxide-modified carbon cloth as cathode for a two-chamber microbial fuel cell', *Nanomaterials*, vol. 6, p. 238, 2016, doi: 10.3390/nano6120238.

[71] R. T. Khajeh, S. Aber, and K. Nofouzi, 'Efficient improvement of microbial fuel cell performance by the modification of graphite cathode via electrophoretic deposition of CuO/ZnO', *Mater. Chem. Phys.*, vol. 240, p. 122208, 2020, doi: 10.1016/j.matchemphys.2019.122208.

[72] D. Z. Khater, R. S. Amin, M. O. Zhran, Z. K. Abd El-Aziz, M. Mahmoud, H. M. Hassan, and K. M. El-Khatib, 'The enhancement of microbial fuel cell performance by anodic bacterial community adaptation and cathodic mixed nickel–copper oxides on a graphene electrocatalyst', *J. Genet. Eng. Biotechnol.*, vol. 20, p. 12, 2022, doi: 10.1186/s43141-021-00292-2.

[73] A. Khandelwal, K. Dhindhoria, A. Dixit, and M. Chhabra, 'Superiority of activated graphite/CuO composite electrode over Platinum based electrodes as cathode in algae assisted microbial fuel cell', *Environ. Technol. Innov.*, vol. 24, p. 101891, 2021, doi: 10.1016/j.eti.2021.101891.

[74] N. A. I. Md Ishak, S. K. Kamarudin, and S. N. Timmiati, 'Green synthesis of metal and metal oxide nanoparticles via plant extracts: an overview', *Mater. Res. Express.*, vol. 6, p. 112004, 2019, doi: 10.1088/2053-1591/ab4458.

[75] N. Nagar and V. Devra, 'Green synthesis and characterization of copper nanoparticles using *Azadirachta indica* leaves', *Mater. Chem. Phys.*, vol. 213, pp. 44–51, 2018, doi: 10.1016/j.matchemphys.2018.04.007.

[76] B. Yuliarto, Yuliarto, W. L. N. Septiani, V. Y. Kanrti, M. Iqbal, G. Gumilar, M. Kim, J. Na, W. C. K. Wu, and Y. Yamauchi, 'Green synthesis of metal oxide nanostructures using natu-

rally occurring compounds for energy, environmental, and bio-related applications', *New J. Chem.*, vol. 43, pp. 15846–15856, 2019, doi: 10.1039/C9NJ03311D.

[77] R. Haripersadh, D. Pillay, and N. Rapiti, 'Impact of rapid centrifugation on routine coagulation assays in South Africa', *Afr. J. Lab. Med.*, vol. 11, p. 1901, 2022, doi: 10.4102/ajlm.v11i1.1901.

[78] L. Feng, X. Tian, Y. A. El- Kassaby, J. Qiu, Z. Feng, J. Sun, G. Wang, and T. Wang, 'Predicting suitable habitats of *Melia azedarach* L. in China using data mining', *Sci. Rep.*, vol. 12, p. 12617, 2022, doi: 10.1038/s41598-022-16571-y.

[79] N. Dharani, G. Rukunga, A. Yenesew, A. Mbora, L. Mwaura, I. Dawson, and R. Jamnadass 'Common antimalarial trees and shrubs of east Africa: a description of species and a guide to cultivation and conservation through use', *World Agroforestry Centre.*, pp. 5-96, 2010.

[80] A. Sen, Sen, A. Batra, and D. V. Rao, 'Pivotal role of plant growth regulators in clonal propogation of *Melia azedarach* L.' *J. Plant Biotechnology.*, vol. 5, pp. 43-48, 2010.

[81] Z. Z. Idrees, and M. A. Mustafa, 'Effect of silver nanoparticles using *Melia azedarach* L. leaf extract on house fly Musca domestica L', *Int. J. Multidiscip. Res. Growth Eval.*, vol. 2, pp. 44–48, 2021

[82] A. Hassan, J. M. M. AL- Doski, and N. Y. M. Ebo, 'Antimicrobial activity of chinaberry *Melia azedarach* extract against pseudomonas syringae PV. syringae in vitro', *J. Univ. Duhok.*, vol. 21, pp. 29–36, 2018, doi: 10.26682/avuod.2019.21.1.4.

[83] D. Sharma and Y. Paul, 'Preliminary and Pharmacological Profile of *Melia azedarach* L.: An Overview', *J. Appl. Pharm. Sci.*, vol. 3, pp. 133-138, 2013, doi: 10.7324/JAPS.2013.31224.

[84] K. Suresh, P. Deepa, R. Harisaranraj, and A. V. Vaira, 'Antimicrobial and phytochemical investigation of the leaves of *carica papaya* L., *cynodon dactylon* (L.) pers., *euphorbia hirta* L., *Melia azedarach* L. and *Psidium guajava* L.', *Core. Ethnobotanical Leaflets.*, vol. 12, pp. 1184–91, 2018.

[85] A. Ahmad, W. A. A. Syed, M. A. Ghufran, Z. Iqbal, and W. H. Shah, 'Green route synthesis of ZnO nanoparticles mediated by *Melia azedarach* for microbiological applications', *Nano Express*, vol. 1, p. 010035, 2020, doi: 10.1088/2632-959X/ab8d11.

[86] G. Chinnasamy, S. Chandrasekharan, and S. Bhatnagar, 'Biosynthesis of silver nanoparticles from *Melia azedarach*: Enhancement of antibacterial, wound healing, antidiabetic and antioxidant Activities', *Int. J. Nanomedicine*, vol. Volume 14, pp. 9823–9836, 2019, doi: 10.2147/IJN.S231340.

[87] K. V. Dhandapani, D. Anbumani, A. D. Gandhi, P. Annamalai, B. S. Muthuvenkatachalam, P. Kavitha, and B. Ranganathan , 'Green route for the synthesis of zinc oxide nanoparticles from *Melia azedarach* leaf extract and evaluation of their antioxidant and antibacterial activities', *Biocatal. Agric. Biotechnol.*, vol. 24, p. 101517, 2020, doi: 10.1016/j.bcab.2020.101517.

[88] G. F. Aaga and S. T. Anshebo, 'Green synthesis of highly efficient and stable copper oxide nanoparticles using an aqueous seed extract of *Moringa stenopetala* for sunlight-assisted catalytic degradation of Congo red and alizarin red s', *Heliyon*, vol. 9, p. e16067, 2023, doi: 10.1016/j.heliyon.2023.e16067.

[89] M. R. Mohammad Shafiee, A. Sattari, M. Kargar, and M. Ghashang, 'MnO_2/Cr_2O_3/PANI nanocomposites prepared by in situ oxidation polymerization method: Optical and electrical behaviors', *J. Appl. Polym. Sci.*, vol. 136, p. 47219, 2019, doi: 10.1002/app.47219.

[90] S. Patade, K. Silveira, A. Babu, F. D'costa, Y. Mhatre, V. Saini, R. Rajput, J. Mathew, R. Birmole, and K. Aruna, 'Bioremediation of dye effluent waste through an optimised microbial fuel cell', *Int. J. Adv. Res. Biol. Sci.*, vol. 3, pp. 214–226, 2016.

[91] Madhusudhana, G. Manasa, A. K. Bhakta, Z. Mekhalif, and R. J. Mascarenhas, 'Bismuth-nanoparticles decorated multi-wall-carbon-nanotubes cast-coated on carbon paste electrode; Electrochemical sensor for sensitive determination of Gallic Acid at neutral pH', *Mater. Sci. Energy Technol.*, vol. 3, pp. 174–182, 2020, doi: 10.1016/j.mset.2019.10.001.

[92] S. A. Akintelu, A. S. Folorunso, F. A. Folorunso, and A. K. Oyebamiji, 'Green synthesis of copper oxide nanoparticles for biomedical application and environmental remediation', *Heliyon*, vol. 6, p. e04508, 2020, doi: 10.1016/j.heliyon.2020.e04508.

[93] V. Mursyalaat, V. I. Variani, W. O. S. Arsyad, and M. Z. Firihu, 'The development of program for calculating the band gap energy of semiconductor material based on UV-Vis spectrum using delphi 7.0', *J. Phys. Conf. Ser.*, vol. 2498, p. 012042, 2023, doi: 10.1088/1742-6596/2498/1/012042.

[94] P. Makuła, M. Pacia, and W. Macyk, 'How To correctly determine the band gap energy of modified semiconductor photo catalysts based on UV–Vis Spectra', *J. Phys. Chem. Lett.*, vol. 9, pp. 6814–6817, 2018, doi: 10.1021/acs.jpclett.8b02892.

[95] E. P. P. Athisayaraj and C. Vedhi, 'Composites of copper oxide and polyaniline for solar cell applications', 2019.

[96] Y. K. Phang, Phang, M. Aminuzzaman, Md. Akhtaruzzaman, G. Muhammad, S. Ogawa, A. Watanabe, and L. H. Tey, 'Green synthesis and characterization of CuO nanoparticles derived from *papaya peel* extract for the photocatalytic degradation of palm oil mill effluent (POME)', *Sustainability.*, vol. 13, p. 796, 2021, doi: 10.3390/su13020796.

[97] F. Ijaz, S. Shahid, S. A. Khan, W. Ahmad, and S. Zaman, 'Green synthesis of copper oxide nanoparticles using *Abutilon indicum* leaf extract: Antimicrobial, antioxidant and photocatalytic dye degradation activitie', *Trop. J. Pharm. Res.*, vol. 16, p. 743, 2017, doi: 10.4314/tjpr.v16i4.2.

[98] S. J. Mokole, A. Aliyu, and O. E. Fayemi, 'Electrochemical detection of dopamine using green and chemical synthesized CuO/PANI nanocomposite modified electrode', *Appl. Phys. A.*, vol. 129, p. 148, 2023, doi: 10.1007/s00339-023-06438-y.

[99] T. O. Abolarinwa, D. J. Ajose, B. O. Oluwarinde, K. P. Montso, J. Fri, O. E. Fayemi, A. O. Aremu, and, C. N. Ateba, 'Antimicrobial properties and cytotoxicity of iron oxide nanoparticles synthesized using *Melia azedarach* leaf extract against diarrhoeal Pathogens', *BioNanoScience.*, 2024, doi: 10.1007/s12668-024-01393-1.

[100] W. W. Melkamu and E. G. Feleke, 'Green synthesis of copper oxide nanoparticles using Leaf extract of *Justicia Schimperiana* and their antibacterial activity', *Research Square.*, pp.1-24, 2022, doi: 10.21203/rs.3.rs-2020143/v1.

[101] A. Abdolahi, E. Hamzah, Z. Ibrahim, and S. Hashim, 'Synthesis of uniform polyaniline nanofibers through interfacial polymerization', *Materials.*, vol. 5, pp. 1487–1494, 2012, doi: 10.3390/ma5081487.

[102] S. V. Joana Sury, A. Ulianas, and S. Aini, 'Synthesis of Conducting Polyaniline with Photopolymerization Method and Characterization', *J. Phys. Conf. Ser.*, vol. 1788, p. 012004, 2021, doi: 10.1088/1742-6596/1788/1/012004.

[103] M. Sawarkar, S. A. Pande, and P. S. Agrawal, 'Synthesis and characterization of polyaniline doped metal oxide nanocomposites', *IRJET.*, vol. 02, pp. 2427-2432, 2015.

[104] W. W. Andualem, F. K. Sabir, E. T. Mohammed, H. H. Belay, and B. A. Gonfa, 'Synthesis of copper oxide nanoparticles using plant Leaf extract of *Catha edulis* and its antibacterial activity', *J. Nanotechnol.*, vol. 2020, pp. 1–10, 2020, doi: 10.1155/2020/2932434.

[105] L. Y. Gemmchu, and A. L. Birhanu, 'Green synthesis of ZnO, CuO and NiO nanoparticles using *Neem leaf extract* and comparing their photocatalytic activity under solar irradiation', *Green Chem. Lett. Rev.*, vol. 17, p. 2293841, 2024, doi: 10.1080/17518253.2023.2293841.

[106] A. L. D. O. F. Rossetto, D. S. Vicentini, C. H. Costa, S. P. Melegari, and W. G. Matias, 'Synthesis, characterization and toxicological evaluation of a core–shell copper oxide/polyaniline nanocomposite', *Chemosphere.*, vol. 108, pp. 107–114, 2014, doi: 10.1016/j.chemosphere.2014.03.038.

[107] D. Zhong, Y. Liu, X. Liao, N. Zhong, and Y. Xu, 'Facile preparation of binder-free NiO/MnO_2-carbon felt anode to enhance electricity generation and dye wastewater degradation performances of microbial fuel cell', *Int. J. Hydrog. Energy.*, vol. 43, pp. 23014–23026, 2018, doi: 10.1016/j.ijhydene.2018.10.144.

[108] J. Hou, Z. Liu, and P. Zhang, 'A new method for fabrication of graphene/polyaniline nanocomplex modified microbial fuel cell anodes', *J. Power Sources.*, vol. 224, pp. 139–144, 2013, doi: 10.1016/j.jpowsour.2012.09.091.

[109] P. P. Rajesh and T. Noori, 'Improving performance of microbial fuel cell by using polyaniline-coated carbon felt anode', *ASCE. J. Hazard. Toxic Radioact. Waste.*, vol. 24, p. 04020024, 2020, doi: 10.1061/(ASCE)HZ.2153-5515.0000512.

APPENDIX I

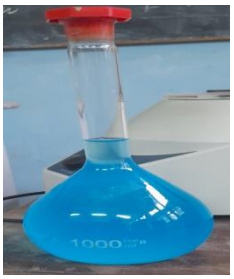

(a) Copper salt solution

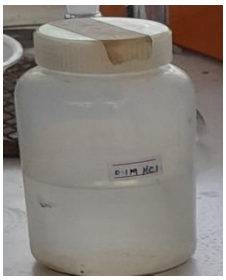

(b) HCl

(c) Aniline

(d) APS

(e) CuO NPs

(f) Polyaniline

(g) CuO/PANI nanocomposite

Figure A1: different chemicals used (a-d) and prepared sample (e-f) in laboratory.

Plastic container

HB pencil

Pencil lead

Copper wire

Digital multimeter

Resistance box

Wastewater sludge

Figure A2: Different materials used for microbial fuel cell construction and voltage measurement

MFC-1

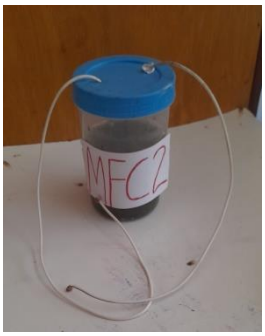

MFC-2

MFC-3

MFC-4

Figure A3: four MFCs Constructed in laboratory

APPENDIX II

Table 6 Table A1 the four constructed microbial fuel cell with their respective electrodes.

MFC	Anode	Cathode
MFC-1	bare PGE	PGE
MFC-2	CuO/PGE	PGE
MFC-3	PANI/PGE	PGE
MFC-4	CuO/PANI/PGE	PGE

Table 7 A2 Row data obtained from closed circuit voltage (CCV) for MFC-1.

Time (min)	Voltage (mV)	Current (mA)	Current density (mAm^{-2})	Power density (mWm^{-2})
0	262	0	0	0
30	230	0.0046	66.34	15.78
60	222	0.0069	100.64	22.25
90	214	0.0084	122.22	26.17
120	207	0.0096	138.75	28.67
150	200	0.0114	165.44	33.05
180	173	0.0136	196.05	33.99
210	168	0.0169	244.20	41.05
240	162	0.0191	276.12	44.73
270	158	0.0213	308.49	48.74
300	151	0.0235	340.14	51.59
330	142.3	0.0259	375.17	53.46
360	133	0.0290	420.43	56.08
390	123.01	0.0346	500.54	61.81
420	113	0.0401	580.21	65.67
450	104.98	0.0440	637	62.16
480	91.24	0.0482	698.40	59.09
510	77.55	0.0523	757.24	56.25
540	69.04	0.0564	816.12	53.19
570	60.2	0.0596	862.8	51.95
600	49.43	0.0658	952.8	47.08
630	40.4	0.0693	1003.1	40.53
660	32.8	0.0719	1041.5	34.17

690	26.5	0.0805	1166	30.91
720	17	0.1786	1282	21.81

Table 8 A3 Row data obtained from closed circuit voltage (CCV) for MFC-2.

Time (min)	Voltage (mV)	Current (mA)	Current density (mAm^{-2})	Power density (mWm^{-2})
0	372	0	0	0
30	349	0.00693	76.03	26.53
60	330	0.0078	98.19	32.5
90	314	0.0112	161.81	50.79
120	296	0.0122	176.92	52.38
150	289.12	0.0154	222.49	64.34
180	282	0.0184	267.07	75.29
210	278	0.0211	306.02	84.76
240	271	0.0236	341.19	92.45
270	264	0.0266	385.14	102.03
300	259	0.0309	446.89	115.41
330	249	0.0344	498.13	124.11
360	243	0.0366	530.1	129.36
390	232.3	0.0404	585.4	136.44
420	206	0.0605	875.17	181.02
450	186	0.0755	1092.26	204.15
480	166	0.0941	1362.7	227.52
510	152.5	0.1117	1618.3	245.96
540	138	0.1287	1862.54	256.22
570	125	0.1474	2134.52	265.75
600	107.7	0.1642	2376.44	251.84
630	76	0.1886	2730.58	208.57

660	54.11	0.2158	3124.61	151.51
690	47	0.2322	3362.8	96.35
720	34.6	0.3461	3563.22	11.88

Table 9 A4 Row data obtained from closed circuit voltage (CCV) for MFC-3.

Time (min)	Voltage (mV)	Current (mA)	Current density (mAm^{-2})	Power density (mWm^{-2})
0	493	0	0	0
30	446	0.0089	128.2	57.56
60	390	0.0128	185.90	72.66
90	372	0.0131	190.24	70.76
120	365	0.0135	195.49	71.43
150	358	0.0171	248.14	88.47
180	351	0.0204	294.91	103.75
210	346	0.0237	340.40	118.52
240	340	0.0267	385.04	131.44
270	336	0.0306	443.65	149.03
300	327.4	0.0335	485.65	158.93
330	318.2	0.0378	545.71	174.01
360	308	0.0413	596.84	184.13
390	298	0.0452	654.89	195.13
420	268	0.0647	936.89	251.01
450	249	0.0797	1150.17	287.21
480	229	0.0976	1415.9	323.52
510	209.4	0.1186	1717	359.54
540	188.4	0.1401	2027.47	382.02
570	147.3	0.1674	2418.07	387.91
600	140	0.1858	2689.7	386.47
630	127.1	0.2162	3130.03	380.41

660	102.5	0.0434	3524.76	346.36
690	81	0.0693	3888.39	215.72
720	39	0.0911	4214.4	50.36

Table 10 A5 Row data obtained from closed circuit voltage (CCV) for MFC-4.

Time (min)	Voltage (mV)	Current (mA)	Current density (mAm^{-2})	Power density (mWm^{-2})
0	451	0	0	0
30	399	0.0097	140.6	56.09
60	391.1	0.0102	148.21	57.96
90	383	0.0112	161.78	61.96
120	375	0.0143	206.99	77.82
150	368	0.0179	258.64	95.43
180	361	0.0212	307.02	111.17
210	358	0.0245	354.01	126.3
240	352	0.0277	401.85	140.85
270	344	0.0314	455.05	156.98
300	338	0.0350	506.78	171.68
330	327.30	0.0386	558.2	183.84
360	319	0.0421	609.56	194.41
390	309.2	0.0460	665.97	205.99
420	279.9	0.0654	947.32	265.19
450	260	0.0804	1164.59	302.81
480	240	0.0984	1424.51	341.88
510	220	0.1194	1728.5	380.27
540	199.7	0.1408	2039.15	407.21
570	158	0.1678	2429.66	416.01
600	140	0.1864	2698.49	414.02
630	130	0.2168	3138.64	407.04

660	109.5	0.2554	3678.73	388.65
690	88	0.2859	4138.72	368.41
720	43	0.3311	4792.19	206.41